

THE EFFECTS OF EVAPORATION RATE, SOLVENT, AND SUBSTRATE
ON THE SURFACE SEGREGATION OF BLOCK COPOLYMERS,

by

Glenn E. Lawson

Thesis submitted to the Faculty of the
Virginia Polytechnic Institute and State University
in partial fulfillment of the requirements for the degree of
Master of Science
in
Materials Engineering

APPROVED:



David W. Dwight, Chairman

James E. McGrath

Garth L. Wilkes

October, 1985

Blacksburg, Virginia

2.2

LD
5655
V855
1985
L387
C.2

THE EFFECTS OF EVAPORATION RATE, SOLVENT, AND SUBSTRATE
ON THE SURFACE SEGREGATION OF BLOCK COPOLYMERS

by

Glenn E. Lawson

David W. Dwight, Chairman

Materials Engineering

(ABSTRACT)

The surface chemistry of two systems of block copolymers was studied using angular dependent X-ray Photoelectron Spectroscopy (XPS). Surface concentration profiles of poly(dimethyl siloxane-b-sulfone)/polysulfone [PDMS/PSF] blends cast at several rates of solvent evaporation, and cast on several substrates were measured. Surface concentration profiles of poly(styrene-butadiene-styrene) [SBS] and poly(styrene-isoprene-styrene) [SIS] triblock copolymers cast at several rates of solvent evaporation, and cast from two different solvents were also measured. The concentration profile analyses were made using three different XPS quantification techniques. The PDMS/PSF systems were analyzed using the peak area ratio, and the SBS and SIS copolymers were analyzed using both the Cls shakeup to main ratio, and spectral measurements of the valence band. The results of this study indicate a variation in surface concentration as well as concentration gradient for different sample preparation routes. The variations can be explained

by considering the rate of film formation (kinetics), polymer - solvent interactions, and polymer - substrate interactions. However, in both systems the lower surface energy copolymer block (siloxane block, or diene block) preferentially segregated to the surface for all of the sample preparation routes studied.

ACKNOWLEDGEMENTS

I wish to extend my sincere gratitude to professor D. W. Dwight for his support and suggestions during the course of this thesis research and my graduate, as well as undergraduate, studies at Virginia Tech. I also wish to thank professor J. E. McGrath and professor G. L. Wilkes for their support during my graduate studies.

I would like to convey my great appreciation to S. McCartney for sharing his knowledge of the X-ray Photoelectron Spectrometer. I would like to thank N. Patel and G. York for inspiring thoughts and comments during my research. I would also like to thank the undergraduate materials engineering students who assisted in some experiments: G. York, J. Kerr, and B. Shaw.

Finally, I thank my wife Robin who is always an inexhaustible source of love and support to me.

TABLE OF CONTENTS

1.0 INTRODUCTION	1
2.0 LITERATURE REVIEW	5
2.1 Bulk Morphology of Block Copolymers	5
2.2 Surface Properties of Block Copolymers	12
3.0 X-RAY PHOTOELECTRON SPECTROSCOPY	20
3.1 Basic Principles	20
3.2 Core Levels	24
3.2.1 Core Peaks	24
3.2.2 Shake-Up Peaks	29
3.2.3 Angular Dependent Analysis	32
3.3 Valence Band	35
3.3.1 Information Content	36
3.3.2 Molecular Orbital Assignments in the Valence Band	39
3.3.3 Quantification of the Valence Band	41
4.0 EXPERIMENTAL	46
4.1 Materials	46
4.2 Methods	50
5.0 RESULTS AND DISCUSSION	54
5.1 Poly(dimethyl siloxane-b-sulfone) System	54
Table of Contents	v

5.1.1 Concentration Profile Versus Evaporation Rate	. 58
5.1.2 Concentration Profile Versus Solvent 61
5.1.3 Concentration Profile Versus Casting Substrate	. 63
5.1.4 General Remarks 69
5.2 Poly(styrene-diene-styrene) system: Shake-up Analysis 70
5.2.1 Analysis of the Component Homopolymers 71
5.2.2 Concentration Profile Versus Evaporation Rate	. 77
5.2.3 Concentration Profile Versus Solvent 78
5.2.4 General Remarks 84
5.3 Poly(styrene-diene-styrene) System: Valence Band Analysis 85
6.0 SUMMARY 105
7.0 CONCLUSIONS 108
8.0 REFERENCES 110
APPENDIX A. NON-LINEAR BASELINE SUBTRACTION PROGRAM	114
APPENDIX B. SILOXANE QUANTIFICATION: EQUATION DEVELOPMENTS 116
VITA 118
Table of Contents	vi

LIST OF ILLUSTRATIONS

Figure 1. Morphology of PS-PI Diblock Copolymer Versus Solvent 10

Figure 2. Schematic Diagram of the Photoelectric Effect 21

Figure 3. Example Spectrum Showing the Various XPS Features. 23

Figure 4. XPS Core Quantification Parameters 27

Figure 5. Schematic Diagram of Angular Dependent XPS 33

Figure 6. Valence Band Spectra of Polyethylene and Polypropylene 38

Figure 7. Effect of Method of Baseline Subtraction . 42

Figure 8. Structure and Characterization of PDMS-PSF System 47

Figure 9. Structure of PS-PD System 48

Figure 10. Characterization of PS-PD System 49

Figure 11. Wide Scan Spectra of PDMS and PSF. 55

Figure 12. Siloxane Concentration Quantification Equations 56

Figure 13. Siloxane Concentration Profile for Various Evaporation Rate. 60

Figure 14. Siloxane Concentration Profile on Clean Mercury. 66

Figure 15. Siloxane Concentration Profile on Water. . 67

Figure 16. Wide Scans of PS, PB, and PI 72

Figure 17. Cls Narrow Scans of PS, PB, and PI 73

Figure 18. Shake-up To Main Ratio Versus Depth for Polybutadiene 74

Figure 19. Shake-up To Main Ratio Versus Depth for Polyisoprene 75

Figure 20.	Shake-up To Main Ratio Versus Depth for Polystyrene	76
Figure 21.	Concentration Profile for SBS Versus Rate of Evaporation	79
Figure 22.	Concentration Profile for SIS Versus Rate of Evaporation	80
Figure 23.	Concentration Profiles for SBS Versus Solvent	81
Figure 24.	Concentration Profiles for SIS Versus Solvent	82
Figure 25.	Valence Band Spectra - SBS	86
Figure 26.	Valence Band Spectra - SIS	87
Figure 27.	MO Assignments for Polystyrene	89
Figure 28.	Pictorial MOs for Benzene	90
Figure 29.	MO Assignments for Polybutadiene and Polyisoprene	91
Figure 30.	Pictorial MOs for Trans-2-Butene	92
Figure 31.	Valence Band Spectra for Toluene Fast Cast - SBS	95
Figure 32.	Valence Band Spectra for Toluene Slow Cast - SBS	96
Figure 33.	Valence Band Spectra for Toluene Fast Cast - SIS	97
Figure 34.	Valence Band Spectra for Toluene Slow Cast - SIS	98
Figure 35.	Relative Peak Heights for the SBS Copolymer	100
Figure 36.	Relative Peak Heights for the SIS Copolymer	101
Figure 37.	Orientation Model For Butadiene Repeat Units at the Surface	102
Figure 38.	Orientation Models For Isoprene Repeat Units at the Surface	103

1.0 INTRODUCTION

Block copolymers are polymers made up of two or more different long blocks of repeat units which are chemically bonded together at one or more locations. If the blocks are incompatible they may separate into phases, each with a high concentration of one block and a low concentration of the other block. Many useful properties of block copolymers arise from their phase separation characteristics and the fact that the different blocks are bonded to each other. The majority of applications of block copolymers have utilized their mechanical properties, which rely on the bulk properties. However, an increasing number of applications are utilizing the variations in surface properties which arise in block copolymers, and blends containing block copolymers.

The main thrust of the mechanical applications of block copolymers has been utilizing (soft) rubbery - (hard) glassy phase separating copolymers. This is the basis of the rapidly expanding thermoplastic elastomer (TPE) market¹. Styrenic TPEs are based on block copolymers of polystyrene with a rubbery polyolefin like polyisoprene or polybutadiene. Some newer classes of TPEs are based on polyester - polyamide block copolymers, polyamide - olefin copolymers block copolymers¹. The general mechanism of elastomer action in these copolymers is that the hard glassy segments act as

physical crosslinks, thus anchoring the rubbery segments between the hard segments. However, at high temperatures (such as processing temperatures) the hard segments melt and thus the polymer can be molded similarly to thermoplastics. Much research has been invested into the effects of processing parameters, polymer composition, block architecture, and block size before TPEs became commercially available, and indeed the research continues still. Other applications of the mechanical properties of block copolymers are the rubber toughening of glassy polymers such as high impact polystyrene (HIPS), poly(styrene-co-acrylonitrile)-g-polybutadiene (ABS), and poly(styrene-co-acrylonitrile)-g-polyolefin (Dow's Rovel).

The applications utilizing the surface properties of block copolymers rely on the ability of the two dissimilar blocks to anchor together two otherwise incompatible surfaces through the block-to-block chemical bond. In an analogous manner several applications use the chemical differences between the blocks to prevent the adhesion. Some applications utilizing the unique surface properties are polyurethane foam stabilizing agents², printing inks³, textile soil-release agents⁴, adhesives⁵, corrosion control⁶, tribology⁷, filler and reinforcement coupling agents. Such applications utilize the variations in surface chemistry attainable with the incorporation of block copolymers due to surface enrichment by one of the blocks. The research into the surface properties

of block copolymers has lagged behind that of the bulk properties. The effects of block size and polymer composition have just recently been investigated, however few, if any, studies have been conducted into the effects of molecular architecture and processing parameters.

Consequently, in addition to the ability to greatly influence the bulk mechanical properties by composition changes, block size, polymer architecture, and processing history, the effects of these parameters on the copolymer surface concentration is also important to understand. The ability to understand and utilize the surface and bulk properties, or perhaps even control them with some degree of independence through variation of those parameters will open the door to more widespread use of block copolymers in existing and new applications.

The present work is focused upon the determination of the surface chemistry of blends of block copolymers, as well as pure block copolymers, which have been prepared using various sample preparation techniques. By utilizing XPS the surface concentration profiles and orientation of the polymer at the outermost surface (top 6.0 nm) has been determined for samples cast at several rates of solvent evaporation, cast from different solvents, and cast on various substrates. It was found that substantial differences in surface concentration and concentration gradients result from the different sample preparation techniques.

In the following chapters a literature review of polymer surfaces is presented, followed by a chapter reviewing aspects of XPS analysis that are related to techniques used in the present work. Then, the actual results and discussion of their meaning is presented.

2.0 LITERATURE REVIEW

This chapter is divided into two sections. The first covers the variations in copolymer bulk morphology due to variations in processing parameters. The second section covers the surface properties of block copolymers. A review of literature more directly related to the XPS techniques used in this study is covered in the next chapter.

2.1 BULK MORPHOLOGY OF BLOCK COPOLYMERS

It has been known for many years that variations in solvent, evaporation rate, as well as other processing parameters can greatly influence the mechanical properties of block copolymers. The influence of those parameters on mechanical (bulk) properties are primary through the alteration of the microphase morphology of the polymer. The effects of process parameters on morphology occurs by either changing the shape of the phase domains, or by changing the purity (i.e. partial phase mixing) of the phases and interphases.

McIntyre and Campos-Lopez⁸ found that small angle x-ray scattering (SAXS) patterns varied for SIS and SBS triblock copolymers cast from different solvents. In particular they found carbon tetrachloride to produce a diffuse interphase between the styrene phase and diene phase. They attributed

this to the fact that CCl_4 is a good solvent for both blocks, thus tending to compatibilize them.

Matsuo and Sagaye⁹ found that the bulk morphology depended upon both the copolymer composition and the solvent used. They found that a rod type, sphere type, or lamellar type domain morphology for SB, BSB, and SBS block copolymers could be obtained by varying the solvent or the overall composition.

Bradford¹⁰ found that even though both toluene and methylene chloride are both non-selective solvents for SB type block copolymers, they gave rise to very different phase morphologies.

Saam and Fearon¹¹ studied the effects of solvent on the morphology and mechanical properties of PS - PDMS diblock and multiblock copolymers. They found that the morphology greatly influenced the mechanical properties. They also found that the effects of solvent on morphology were greater for the diblock than for the multiblock copolymer. In general, they found that a preferential solvent for one block tends to make that block the dominant phase on a volume basis. This is a result of the good solvent causing the compatible block chain segment to expand (i.e. to increase its root mean square end to end distance) during the casting period, while the non-compatible block chain segment compresses. Thus the authors could make a morphology of cell-like domains of PS in a PDMS matrix by casting from

cyclohexane (selective to PDMS), or they could produce the inverse morphology by casting from styrene (selective to PS).

Recently, Bajaj, et al.¹² studied the effects of solvent on the morphology of PDMS-PS-PDMS triblock copolymers blended in PS homopolymer. They found that two types of morphology resulted from the use of a non-selective solvent (toluene) and a PS selective solvent (THF). The morphology of the THF cast film showed the PS midblock solubilized in the PS homopolymer (the major component). Thus producing a morphology of siloxane-block domains in a PS matrix. The morphology of the toluene cast film showed domains of block copolymer in a PS matrix. Their explanation was that the preferential solvent caused improved mixing of the PS blocks and homopolymers while compressing and separating PDMS blocks. A non-selective solvent made the entire block copolymer chain expand which was incompatible with PS homopolymer, thus the entire block copolymer phase separated.

Similar behavior was observed on the SBS system cast from a variety of solvents with different solubility parameters by Bagrodia and Wilkes¹³. They found that Young's modulus of elasticity increased as the solvent's solubility parameter increased to values close to that of PS. They found this behavior to be generally occurring over the range of 10% to 75% PS (varying the block copolymer PS content), but it was most pronounced at 30% PS. The modulus increased with solubility parameter because the PS blocks swelled more and re-

mained in solution longer than the PB blocks, hence they formed the continuous phase. Since the modulus is measured from the initial part of the stress-strain curve it is strongly influenced by the continuous phase. Thus as the continuous phase changed from PB to PS the modulus increases greatly.

However, Bates, et al.¹⁴ found that the primary effect of solvents on SB diblock copolymer blend morphology was in the domain dimensions. They found that the PB domain morphology of the SB blended into PS films changed from cylinders to spheres as the solvent was changed from toluene to THF/MEK (70:30). However, they found that the neat diblock films did not vary in domain structure. PB spheres were present whether the film was cast from toluene, benzene, or THF/MEK. They noted that this was consistent with findings by Hashimoto, et al.¹⁵ and Pico and Williams¹⁶. Pico and Williams stated that the volume fraction of PS (which depends upon the PS chain dimensions) would not vary much with solvent, as long as the solubility parameter was in the range suitable to both component blocks.

Molau, et al.^{17, 18} explained the effects of solvent on morphology based on the colloidal properties of SB diblock copolymer solutions. They found that depending upon the solvent, micelles with PS cores or PB cores could be formed. A PS core results when a solvent preferential to PB is used, and visa versa.

Inoue, et al.¹⁹ studied the effects of both solvent and initial solution concentration on the resulting domain morphology of SI diblock copolymers. They found that the size of the domains varied with the solubility parameter of the solvent. In this case, a poor solvent for PS but a good solvent for PI caused the PS domains to become irregularly shaped and smaller, see inset "d" on Figure 1. Note that in the figure the insets "a" to "d" are in order of increased PI selectivity of the solvent. These researchers also disproved a theory presented by several other researchers which stated that the final morphology depended upon the initial solution concentration. Their work showed that as long as a true solution was made (that is, the polymer concentration is below its critical point), the final morphology was the same. They postulated that the morphology is determined as the polymer precipitates and is independent of the initial concentration. They, however, did not address the issue of the effect of the rate of precipitation on the morphology.

Dawkins²⁰ studied the morphology resulting in SIS block copolymers and found that the rate of solvent evaporation also affected the morphology. He noted that toluene cast SIS copolymers had uniformly sized and spaced spherical PS domains. However, as the evaporation rate increased the domains became less well separated. Dawkins²¹ made the general comment that slowly evaporated films contain equilibrium domains. The domain boundaries also become more and more

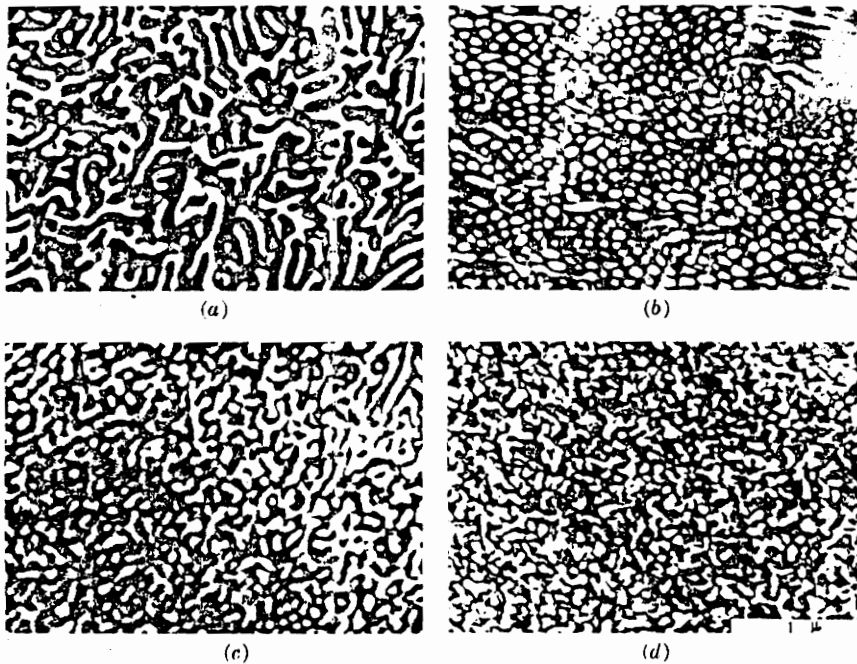


Figure 1. Morphology of PS-PI Diblock Copolymer Versus Solvent : TEM Photomicrographs of films cast from 2.5% solutions of 40/60 PS/PI diblocks in (a) MEK; (b) cyclohexane; (c) CCl_4 ; and (d) heptane. (From Inoue¹, page 1289).

sharp. Quickly cast films had ill-defined morphologies and in this respect resembled compression or injection molded films.

Noshay and McGrath^{2,2} in their overview book covering much of the block copolymer science prior to 1977 briefly discussed the effects of evaporation rate on SBS block copolymers. Rapidly evaporating the solvent produced a lamellar domain structure, while slowly evaporating the solvent produced spherical PS domains in a PB matrix. They also noted that compression molded films had bulk morphologies similar to those of rapidly evaporated films.

Cohen and Bates^{2,3} worked with both varying the solvent and the evaporation rate for polyisoprene / poly(n-butylmethacrylate) [PI/PBMA] diblock copolymers. They observed that a fast rate of solvent evaporation caused larger domains to be formed near the sample surface. These domains contained phase-mixed diblock copolymer which froze-in-place as the solvent evaporated before binodal phase separation could occur. These domains were not observed in the center of the sample because the solvent evaporation rate there was much slower. They found that the large domains disappeared when the film was annealed or when solvent was added to the film. This led them to the conclusion that the large phase mixed domains at the surface were thermodynamically unstable or metastable. They also found that the minor phase morphology of the slow cast films varied from rods to unduloids to

spheres as the solvent progressively became a good solvent for both blocks.

Thus it is clear that the bulk morphology of block copolymers is very dependent upon processing parameters. The solvent and evaporation rate both effect the domain shape and spacing, as well as domain boundary sharpness. It is clear from the literature that the slower the solvent evaporation the closer the approach to equilibrium phase domain morphology. However, if two films cast from different solvents can have different morphologies, it follows that slowly cast films from different solvents can have different morphologies. Therefore, once the solvent is totally evaporated the films then will rearrange (at perhaps a very slow rate, determined by diffusion), to a true equilibrium morphology. Nevertheless, even though the post-processing morphology is not an equilibrium one, it may be sufficient long-lived for its unique properties to be measured and utilized.

2.2 SURFACE PROPERTIES OF BLOCK COPOLYMERS

There have been several methods used to analyze the surface properties of block copolymers. Many of the first studies measured the surface tension, some also used adhesion or SEM replication of the surface, while more recent studies have used XPS.

LeGrand and Gaines²⁴ used contact angles to determine that PDMS-PC (polycarbonate) block copolymers surface segregated in PC blends. They found that the contact angle of the blend with as little as 0.1% by weight block copolymer was close to the contact angle of pure PDMS. They found this behavior to be independent of siloxane block size for the polymers they studied (block size of at least 1500 g/mol). They attributed the surface segregation to the much lower surface energy of the siloxane block. Continuing along those lines Gaines, et al.^{25, 26} studied the surface segregation of block copolymers as a function of composition and temperature (a key diffusion parameter). They found that for PDMS-PS blended into PS the surface was dominated by PDMS blocks even for blends with as little as 0.2% by weight block copolymer. However, they found that the surface tension changed with time and temperature. They made the remark that when the low surface energy blocks are long enough and insoluble in the solvent they will concentrate at the surface. They also found that very low concentrations of block copolymers could bring about large changes in the surface properties. A similar behavior was found by Owen and Thompson⁷ who observed siloxane surface segregation in a blend of polycaprolactam-PDMS block copolymer in nylon-6.

Prompted by those studies Kagen, et al.⁵ and Kaelble, et al.²⁷ studied the adhesion properties of block copolymers. Kagen, et al. found that additions as low as 0.1 wt% of a SBS

block copolymer, (very similar to the one used in the present study, at 80,000 MW and 28% PS), to either vulcanized PB (v-PB) or PS decreased the polymer surface tension. They attribute this to the surface segregation of the block copolymer based on bulk incompatibility. Using the fact that the copolymer dominated the surface they formed thermal bonds between PS and v-PB, one of the films contained the blended block copolymer. They found a large dependence of the peel strength on block architecture and copolymer concentration. Increasing the block copolymer concentration increased the degree of interpenetration and hence increased the bond strength. They also found that 80,000 MW diblock copolymer (15% PS) blended into v-PB produced weaker thermal bonds to PS than an 80,000 MW triblock copolymer (28% PS) blended into v-PB. They did not discuss this point but this author would expect the fact that the triblock has twice as many PS chain ends as the diblock to be an important factor.

Kaelble, et al.²⁷ found that neat SBS triblock copolymer when bonded to another SBS film had significant thermal bond strength development at low temperatures. They found that at temperatures as low as 50°C (after 15 minutes bonding time) a substantial bond strength had developed. Since this is some 40° to 60°C below the glass transition temperature of PS, the bond strength is probably the result of cross-diffusion of PB domains, thus requiring at least some PB domains to be present at the surface.

Yamashita²⁸ studied PS-poly(THF) [ST] diblock copolymers, STS triblock copolymers, and blends of these in PS and PTHF. He found two important features using surface composition measurements. The first was that for neat block copolymers the surface concentration (measured on OsO₄ stained TEM films) varied such that the minor component surface segregated. He attributed the unexpected PS surface segregation to expulsion of PS from the bulk as the PTHF blocks crystallized. The second point of interest was derived from his surface tension experiments on melts of blends. He found that in all cases the THF block surface segregated even for PTHF blended with ST copolymer. Thus he concluded that merely being incompatible with the major bulk phase could not overcome even a modest (3 dyne/cm in this case) surface energy driving force. However, large magnitude forces such as crystallization expelling the dissimilar block could override the surface energy driving forces. Thus he made the important conclusion that the surface concentration of block copolymers depends upon the interplay of several driving forces.

Bradford and Vanzo²⁹ as part of their research used replica SEM to study the morphology of the surface of SB diblocks copolymers. The surface replicas they obtained showed that the surface morphology was of the same type of morphology and of the same size as the bulk morphology. Their replicas also showed that the surface had a rough tex-

ture. However, it should be noted that several areas on the replicas showed no texture whatsoever, this could be due to a replica preparation problem or actual large areas on the sample which are covered with one type of domain. Surface roughness was also observed³⁰ in the PS/PEO (polyethylene oxide) diblock copolymer system which showed PS globules and fibrillar PEO domains.

The surface chemistry of PDMS-PC perfectly alternating block copolymers and their blends were studied by XPS by J. S. Riffle, J. E. McGrath, D. W. Dwight, et al.³¹⁻³³. They found that the neat copolymer had PDMS surface segregation for all cases studied, but the surface concentration of PDMS depended upon the block copolymer siloxane content and block size. For siloxane contents of 8 to 33% with block size of 1800 g/mol the surface concentration of siloxane was 60%. However, for siloxane contents of 41 to 70% with block sizes of at least 5000 g/mol the surface concentration was 82 to 94% siloxane. They also found that for a fixed siloxane content increasing the block size increased the siloxane surface concentration. Blends of these copolymers in polycarbonate were found to have a predominately siloxane surface, even at bulk concentrations as low as 0.05% siloxane. They found the blend's surface concentration of siloxane to have a sharp break at about 1% siloxane in the bulk. Below 1% the surface concentration was about 10% for thin chloroform cast films, and 30% for thick pressed films.

Blends with more than 1% siloxane had surface concentrations of about 70% for thin chloroform cast films, and 50% for thick pressed films.

Sha'aban³⁴ studied the surface composition of PDMS-polyurethane block copolymers and blends with segmented polyether-urethane using XPS. He found that the neat block copolymer had a surface composed entirely of siloxane blocks. The siloxane surface concentration of blends exhibited an abrupt increase at a bulk block copolymer content of 1 to 11%. Blends containing more than 11% block copolymer had surfaces of entirely PDMS blocks, while blends containing less than 1% block copolymer had siloxane surface enrichment, but urethane segments were also detected.

The most systematic recent study of block copolymer surface concentration was performed by Thomas, O'Malley, et al.³⁵⁻³⁷ in a series of three papers covering the PS-PEO (polyethylene oxide) system. They studied blends of PS and PEO, PS/PEO diblock, and PEO/PS/PEO triblock copolymers. Their study of blends³⁵ showed that the PS surface segregated (PS has the lower surface energy) and the film formed a laterally inhomogeneous surface domain morphology. Their results also indicated some phase mixing which they expected to be small due to the crystallization of PEO and the PEO-PS incompatibility. Their study of PS/PEO diblock copolymers³⁶ also contained a study of the effects of the casting solvent. They found that the surface concentration of block copolymers

with varying PS composition did vary with different solvents. In all cases PS segregated to the surface more readily in a PS selective solvent than in a non-selective solvent, or a PEO selective solvent. They also found that the diblock surface segregation was greater for a given bulk PS composition than in the blend case. In addition, they found that the PS domains at the surface were raised slightly above the surface plane, giving rise to surface texture. In all cases of varying PS compositions and casting solvents they found that the PS surface segregated. Their study on PEO/PS/PEO triblock copolymers³⁷ supported their findings for the diblock case.

In summary, the studies of block copolymer surfaces to date shows several factors which may be applicable to other phase separating block copolymers and their blends. The lower surface energy block will tend to surface segregate. The actual surface concentration will depend upon the interplay of several driving forces. Block copolymers also appear to have a surface which has a inhomogenous phase morphology which may be related to the bulk morphology.

It is interesting to note that none of the literature reviewed contained enough information regarding sample preparation to allow reproducing the experiments. Since several studies contained non-equilibrium bulk and surface morphologies, some measure of the rate of solvent evaporation

should have be stated. This would permit other experimenters to reproduce the experiments and obtain similar morphologies.

3.0 X-RAY PHOTOELECTRON SPECTROSCOPY

Since X-ray Photoelectron Spectroscopy (XPS) has so often been used for the chemical analysis of surfaces, all of the general principles of the techniques will not be discussed in length. However, certain aspects of XPS and the analysis of the spectra which are relevant to this study will be reviewed below.

3.1 BASIC PRINCIPLES

XPS is the study of the kinetic energy and the corresponding intensity of electrons ejected from an irradiated sample by the photoelectric effect. The photoelectric effect is shown schematically in Figure 2. When a photon of sufficient energy is absorbed by the electron it can attain enough kinetic energy to overcome the binding energy forces of the atom and be ejected. A XPS instrument measures the kinetic energy of electrons which have enough energy to leave the surface of the sample. The binding energies of the electrons can then be computed from the photon energy (1253.6 eV in the present study), and a small correction for sample charging and the instrument work function.

Along with the ejection of photoelectrons several processes can take place, the Auger effect, shake-up, and shake-

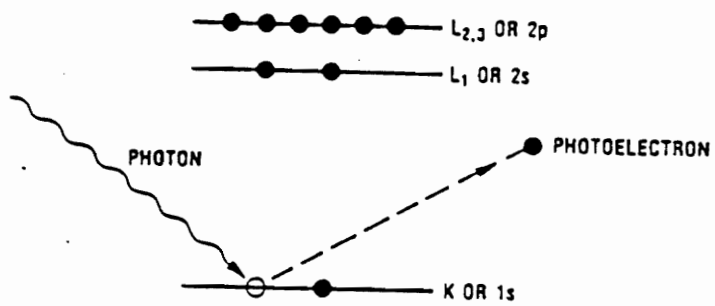


Figure 2. Schematic Diagram of the Photoelectric Effect: (From D. Briggs³⁸)

off. When a photoelectron is ejected from a subshell, thus ionizing the atom, it leaves behind a hole (i.e. a charge deficiency). The Auger effect is the filling of this hole by an electron from a higher level orbital, with the simultaneous ejection of another electron. Shake-up and shake-off are valence band transitions which accompany core level photoionization. Both result from the change in effective atomic charge, resulting from photoionization, which affects the valence electrons. Shake-up is the transition from an occupied valence level to an unoccupied one. Shake-off is the ionization of an electron from an occupied valence level.

The XPS spectra, therefore, contain many features indicative of the chemistry of the sample surface. For each element present there are Auger peaks, shake-up peaks, core peaks (from the main photoelectric effect), shake-off peaks, and valence peaks. Some of these features are marked on the example spectrum shown in Figure 3. The areas of the spectrum utilized during the present study were the core peaks, the shake-up peaks, and valence peaks. Auger peaks and shake-off peaks are generally difficult to interpret, and were not utilized in this work.

3.2 CORE LEVELS

As indicated in the previous section core peaks arise from the electron ejection which is the primary photoelectric

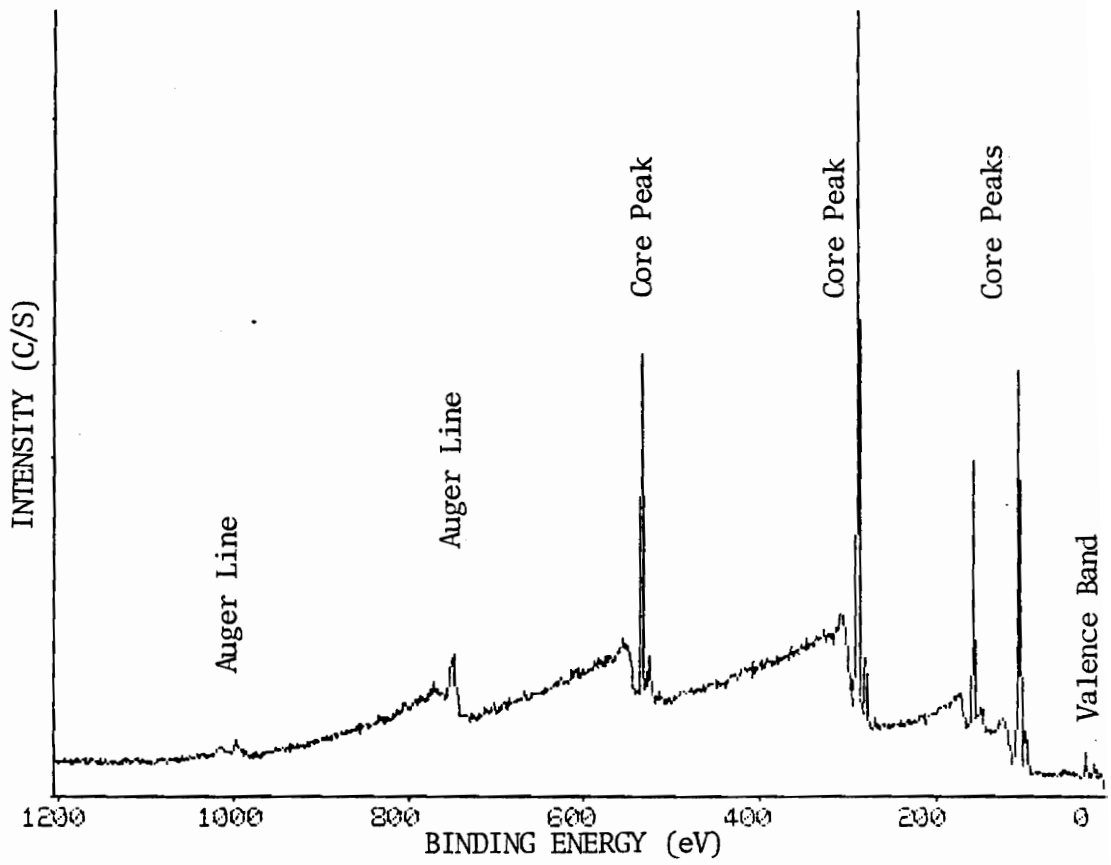


Figure 3. Example Spectrum Showing the Various XPS Features.

process. Since shake-up is a secondary photoelectric process but intimately related to the core peak, both processes will be discussed in this section.

3.2.1 CORE PEAKS

The core peak has long been used as the primary route to qualitative, as well as, quantitative chemical analysis of the surface. The core peaks are the most suited to chemical analysis, being the dominant features on a XPS spectrum, (and consequently they were the first to be used in quantitative analysis). The intensity of a core peak depends upon many instrument and material variables which are hard to determine. Thus quantification is based upon the ratio of two core peak areas (the area under the peak being the integral of the number of photoelectrons detected in a small interval about the binding energy of the core peak). When the area ratio technique is used all but three factors cancel out. The three factors remaining are the photoelectron inelastic mean free path (IMFP), the sub-shell photoionization cross-section (SPC), and the spectrometer transmission function.

The physical representation of IMFP is the distance that an ejected photoelectron can travel before an inelastic collision. More precisely it is the distance that electrons can travel with a $1/e$ chance of avoiding inelastic collisions. Since an inelastic collision causes the photoelectron to lose

kinetic energy, an inelastic collision causes the photoelectron to appear as though it had a higher binding energy, and it will either broaden the main core peak or appear as background noise. Consequently, the IMFP is a measure of the depth from which photoelectrons can escape the sample and be counted under the main core peak. The IMFP values have long been under dispute by many workers in the field. In 1979 C. D. Wagner, et al.³⁹ presented a plot of IMFP versus photoelectron kinetic energy for a variety of elements which fit a single equation fairly well (for kinetic energies above 300eV). This plot was based upon a tabulation presented by C. J. Powell⁴⁰. The relationship he proposed was that IMFP is proportional to the photoelectron kinetic energy raised to the 0.75 power. Both before and after Wagner's work others had proposed exponents which ranged from Castle's⁴¹ 0.5 to Clark's⁴² 2.22. However, in 1981 J. Szajman, et al.^{43, 44} developed an equation for the IMFP based on the dielectric theory and equations developed by Powell. They found that theory, as well as the majority of the most accurate experimentation (Powell⁴⁰ and Penn⁴⁵), supported the 0.75 exponent. The proportionality constant, they found, was material dependent and was expected to vary greatly with changes in the electronic structure of the sample. Since all of the samples studied in the present work are organic non-conducting polymers, the IMFP values used in the present work are based on the 0.75 exponent and a proportionality constant

of 0.1048 (when IMFP is in Ångstroms and photoelectron kinetic energy is in eV). This value of the constant is the value derived from Wagner's data. The resulting IMFP values for the core peaks of interest in the present work are shown in Figure 4. It can be shown^{4,6} that 63% of the no-loss photoelectrons leaving the sample are from up to $1 \cdot \text{IMFP}$ deep. However, the depth of the sample from which 95% of the no-loss photoelectrons arise is $3 \cdot \text{IMFP}$ deep. Consequently, $3 \cdot \text{IMFP}$ can be used to estimate the depth of analysis into the sample. As one can see the IMFP values are all very small, about 2 nm, this makes XPS a very surface sensitive chemical analysis tool (analyzing the top 6 nm of the sample).

The physical representation of SPC is the cross-section (or target area) that a sub-shell electron presents to photons of a certain energy. Hence, the larger the value, the larger the probability of a photon-electron interaction and subsequent photoionization. Unlike the IMFP, the SPC values have not been the subject of much debate and the values generally accepted today are essentially the same as those first presented by Scofield^{4,7} in his comprehensive 1976 tabulation. In general, the differential SPC^{4,8} must be used for quantitative analysis. The differential SPC is a product of the total SPC (as tabulated by Scofield) and a term which is a function of the asymmetry parameter and the angle between the axis of the X-ray beam and the axis of the energy analyzer. However, the instrument used for this work is

Core Peak	(A) Kinetic Energy (eV)	(B) IMFP (nm)	(C) SPC (kilobarns)	(D) $= (A) * (B) * (C) * 10^{-3}$ (barns * eV * Å)
Cl _{1s}	967	1.82	22.2	390
O _{1s}	723	1.46	63.3	668
Si _{2p}	1151	2.07	19.2	317
Si _{2s}	1101	2.00	19.0	418
S _{2p}	1088	1.99	38.6	835
S _{2s}	1025	1.90	27.8	540

Figure 4. XPS Core Quantification Parameters

oriented such that the angle between the axis of the X-ray beam and the axis of the electron energy analyzer is the magic angle of 54.6° . At the magic angle the asymmetry parameter term is one, hence no modification of the SPC values due to asymmetry was needed in the present work. Scofield's SPC values for the core peaks of interest in this work are shown in Figure 4. Note, however, that the SPC value for Si2p was found to be inconsistent with several experiments in the current work. Hence, a new value of 21.1 kilobarns was calculated and used for quantitative analysis. The specifics of this inconsistency are discussed later in the Results and Discussion Chapter, PDMS/PSF System Section.

The final factor needed to perform quantitative analysis of XPS spectra is the spectrometer transmission function. The transmission function is an instrumental correction factor which accounts for the effects of photoelectron retardation and efficiency losses in the detector system. In the present work the XPS was operated in the Fixed Retardation Ratio (FRR) mode which retards the photoelectrons to a fixed fraction of their initial kinetic energy before they enter the energy analyzer. For this mode of operation the transmission function is proportional to the photoelectron kinetic energy. The constant of proportionality drops out of quantitative chemical analysis when peak area ratios are used, consequently the kinetic energy can be used as the trans-

mission function. The kinetic energy for the XPS peaks of interest in the present work are shown in Figure 4.

As stated above, an area ratio can be converted into an atom ratio by accounting for the IMFP, SPC, and transmission function. Atom fractions of elements are inversely related to the product of these three factors. Therefore, these three factors can be collected into one product which has the values shown in the last column of Figure 4. The larger this factor the more intense the spectral peak will be for a given atom fraction.

3.2.2 SHAKE-UP PEAKS

Shake-up peaks are present on the low kinetic energy side of core peaks and are theoretically always present, however they are not always intense enough to be observed on the spectrum^{4,6}. Shake-up peak analysis has only occasionally been used for qualitative or quantitative chemical analysis. The primary reason for the lack of activity on shake-up analysis is the low intensity of the peaks (normally inseparable from background noise), and the usual presence of more intense and easily handled core peaks from each element. However, in some instances, as in wholly hydrocarbon polymers, there is only one element giving rise to core peaks (hydrogen does not give rise to a detectable XPS peak). This was the case in the polystyrene-b-diene system. Fortunately,

polymers containing pi-bonds have shake-up peaks of much greater intensity than saturated polymers. Furthermore, the shake-up intensity is much greater for polymers containing aromatic pi-bonds than polymers containing a single pi-bond per repeat unit (i.e. no conjugation). Consequently, it seems that the concentration of styrene and diene repeat units could be readily determined from analysis of the Cls shake-up to main peak area ratio.

D. T. Clark, et al.^{49, 50} studied perfectly alternating alkane-styrene copolymers by using the Cls shake-up to main peak area ratios to determine surface concentration profiles. They noted that the alkane segments (made up of $-CH_2-$ repeat units) are fully saturated and hence do not contribute noticeably to the observed shake-up intensity. On the other hand, styrene contains conjugated unsaturation which gives rise to a relatively intense shake-up peak. Clark, et al.⁴⁹ showed that the shake-up phenomena is localized on the component which contains the pi-bonds, and they noted that the shake-up peak in alkane-styrene copolymers might be additive. As a result of this argument, and the use of its results, the qualitative surface concentration profile was constructed. Clark, et al.⁵⁰ used the analysis of the qualitative profile to show that alkane units segregated to the copolymer surface. Clark, et al.^{51, 52} also showed that the shake-up intensity is greatly dependent upon the degree of substitution of the aromatic ring on polystyrene. They found PS to have

the higher shake-up probability and aromatically substituted PS to have a lower shake-up probability. Thus the electronic environment bonded to the ring can alter the valence band of the ring enough to alter the shake-up probabilities. J. J. O'Malley, et al.³⁷ used the Cls shake-up to main peak area ratios to prove phase mixing of polyethylene oxide and polystyrene occurred at the surface of PEO/PS copolymers. They proved this by observing a decrease in shake-up intensity which was due to the electronic environment (the phase mixed polymer interacting with the valence band of the PS ring). The surface concentration profile in this case was established by using the Cls to O1s area ratio. Nonetheless, the work by Clark, et al. has formed the basis of quantitative shake-up analysis of purely hydrocarbon polymers which contain unsaturation. Neither of these investigators discussed the angular dependent spectra of their homopolymers, they assumed uniform composition within the XPS sampling depth.

In the present work the basic principle stated by Clark et al. was used and expanded upon. Expansion was needed because both styrene and diene blocks contain unsaturation. The assumption was made that the shake-up phenomena in diene repeat units were localized in the pi-bond location, as they are in polystyrene. This is a reasonable assumption since the electrons and orbitals which cause the shake-up phenomena are localized in the one diene pi-bond location, and are much

more localized than the electrons and orbitals that give rise to the shake-up phenomena in polystyrene. Since the shake-up is localized to each repeat unit, shake-up peak intensities are additive. Consequently, quantitative equations can be developed to express the relative amounts of diene and styrene once the Cls shake-up to main area ratio for the corresponding homopolymers are known. However, as will be seen, the shake-up to main ratio of the homopolymers varies with angle and processing parameters. Consequently, in the present study only the shake-up to main area ratio will be used to semi-quantitatively measure concentration. The higher the ratio, the higher the pi-bond concentration, or the higher the styrene concentration.

3.2.3 ANGULAR DEPENDENT ANALYSIS

A schematic diagram of the angular dependent experiment is shown in Figure 5. As the sample surface tangent rotates toward the energy analyzer axis the depth of analysis decreases. In order to get the same degree of photoelectron attenuation due to inelastic collisions, the electrons must travel the same distances through a homogeneous material. Therefore, as the take-off angle decreases from 90° the depth of analysis into the sample (measured normal to the sample surface) decreases. The fraction of electrons leaving the

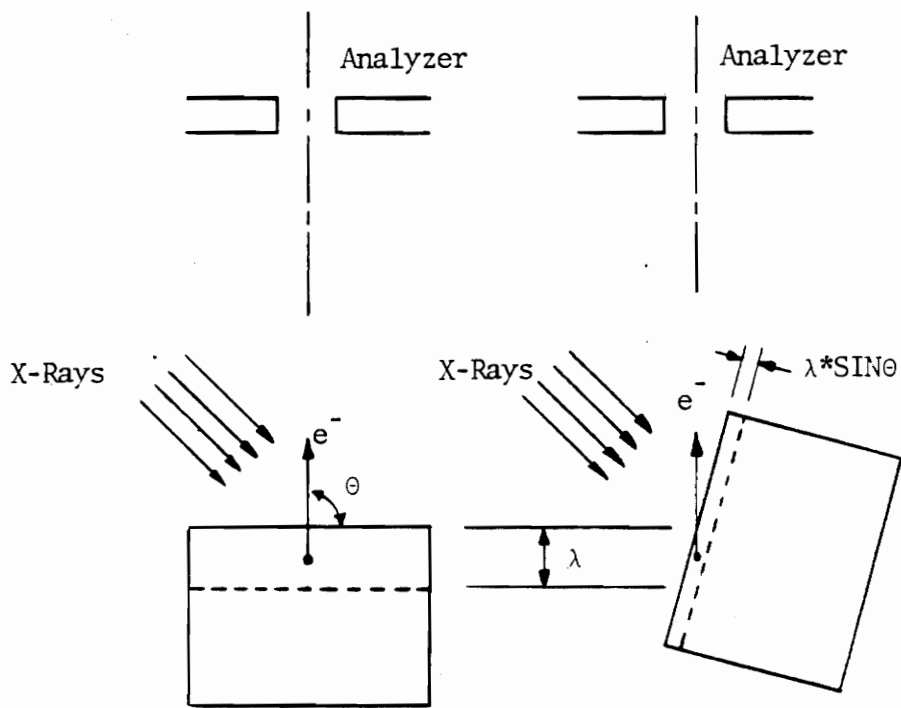


Figure 5. Schematic Diagram of Angular Dependent XPS

sample without suffering an inelastic collision is given by the equation below:

$$F = C * \exp (-x / (\lambda * \sin\theta))$$

Where: C = constant; x = depth into the sample (measured normal to the sample surface) from which no-loss electrons can be emitted; λ = IMFP; and θ = angle between the sample surface tangent and the analyzer axis. By setting F to some fixed value, x can be determined. In the present work the angle θ was used as a depth measurement, however x could just as easily been used. Over 95% of the photoelectrons emitted are generated within $3 * \text{IMFP}$ of the surface (relative to analyzer axis). Consequently, using this as the criterion to scale the depth x would assume the values of 5.46 nm, 2.73 nm, and 0.96 nm for $\theta = 90^\circ$, 30° , and 10° , for Cls photoelectrons respectively, enabling an analysis of the concentration versus depth profile of the sample surface.

Two features of the angular dependent experiment make it difficult to quantify. The first feature that makes the angular dependent results semi-quantitative are differences in IMFP of different elements. Hence, if elements with greatly differing binding energies (and therefore IMFP) are used to determine the concentration, the results may be slightly erroneous. For instance, using Cls and Si2p peaks to form a concentration ratio at 90° really results in a ratio of the carbon in the top 5.46 nm to the silicon in the top 6.21 nm (a 14% depth error). The error due to large differences in

core level binding energy, of course, increases as the concentration gradient becomes steeper. During the present work some experiments were performed using S2p and Si2p ratios which would result in a depth of analysis error of 0.24 nm (4% error) at 90°. The remainder of the work on core levels was conducted by analysis of the S2p to Si2s, or Cls to shake-up ratios, in both of these cases the binding energy difference is very small. As a consequence the concentration analysis was performed on essentially the same depth into the sample. The second feature preventing quantification of the angular dependent analysis is the effect of surface roughness (topographically rough or density variations). The major effect of surface roughness is to cause shadowing of photoelectron emission by surface asperities. Another effect is the varying angular orientation (local surface tangent to analyzer axis) which varies greatly over the rough sample surface.

3.3 VALENCE BAND

Valence band peaks arise from the photoionization of valence level electrons. This is contrasted to core levels which are the tightly held innermost orbitals. The valence band is of particular interest since it is the valence electrons which are most affected by variations in the chemical bonding environment. However, the various molecular

orbital energy levels are very close together in binding energy. This causes serious peak overlapping and makes it difficult to resolve valence band spectra. However, as discussed below, information on a qualitative and semi-quantitative level can be obtained from the analysis of the valence band.

3.3.1 INFORMATION CONTENT

There have been several investigators who have used analysis of the valence band to demonstrate its information content. The two principal investigators in the field of valence band photoelectron spectroscopy of polymers have been J. J. Pireaux, et al. who used XPS and molecular orbital (MO) models, and W. R. Salaneck who used XPS, UPS (Ultraviolet Photoelectron Spectroscopy), and MO models.

Pireaux, et al.^{53, 54} showed that XPS of the valence band could reveal polymer chemical and physical differences as subtle as tacticity or crystalline forms. The greater the chemical or physical difference, the greater their effect on the molecular orbitals and the greater the difference of the valence band spectra. They showed that the valence band spectra for polypropylene and polyethylene were vastly different due to the presence of the additional methyl side group on the polypropylene repeat unit. Their polyethylene and polypropylene spectra are presented in Figure 6 which

clearly shows the methyl peak for polypropylene. These differences are also expected to be observed between the valence band spectra of polybutadiene and polyisoprene. They had thus demonstrated that the valence band could be used to analyze wholly hydrocarbon polymers that did not necessarily contain pi-bonds.

Salaneck⁵⁵ has shown the differences encountered between UPS, XPS, and MO calculations. Due to the cross-section differences for photons of ultraviolet energy and X-ray energy, substantial differences result in the experimental spectra. In general an UPS spectrum will have an enhanced C2p region, (10 to 0 eV range), while a XPS spectrum will have an enhanced C2s region, (20 to 10 eV range). This feature makes UPS the most sensitive method since the C2p peaks are even more responsive to the chemical environment than the C2s peaks. Nonetheless, XPS has two distinct advantages over UPS. The first advantage of XPS is the ability to collect the valence band and the core levels. The second advantage is the much greater depth of analysis of XPS which reduces the effects of surface oxidation and contamination on the spectra. Salaneck has used valence band UPS to differentiate between cis and trans polyacetylene. Furthermore, he has used a simple weighted average quantification routine to determine the amounts of cis and trans. (As will be discussed later, XPS is not as sensitive to cis- and trans-stereoisomeric differences.)

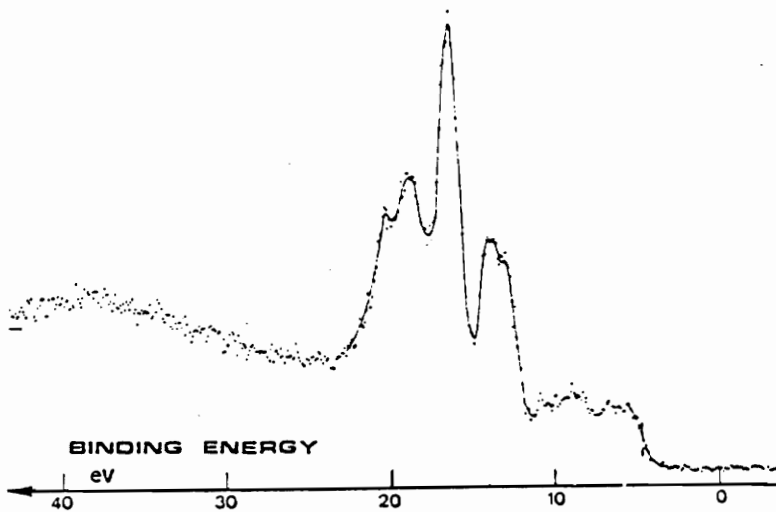
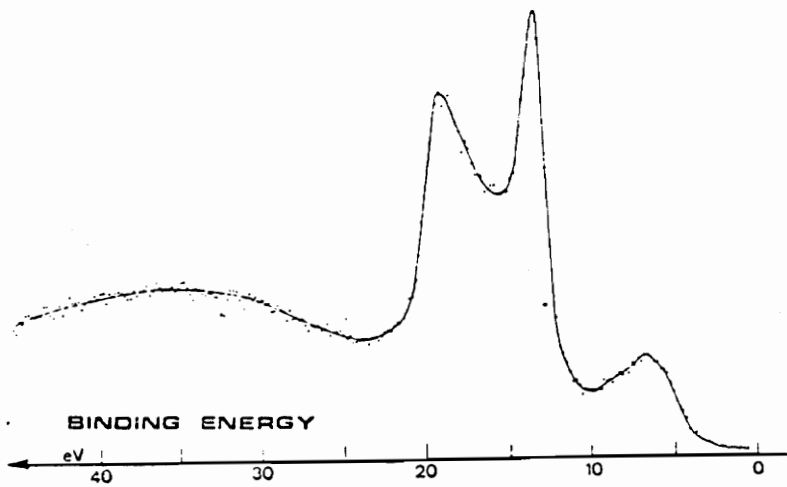


Figure 6. Valence Band Spectra of Polyethylene and Polypropylene: (From Pireaux, et al.⁵⁴ pages 332 and 334).

Consequently, the valence band as measured by UPS or XPS can reveal great detail into the structure of a polymer. Analysis of the spectrum can also be used to quantitatively delineate between hydrocarbons with small chemical differences. This is the reason the analysis of the valence band was undertaken in the present study. By analysis and comparison of the spectra it was hoped that verification and clarification of the results of the shake-up to main ratio could be obtained.

3.3.2 MOLECULAR ORBITAL ASSIGNMENTS IN THE VALENCE BAND

The key to understanding the full detail of the valence band is assignment of the many peaks in the band. The method of MO assignment used for polymer analysis is to assign peaks based upon model compounds which are similar or have the same dominant functional groups as the polymer repeat unit. Pireaux, et al^{53, 54} have made MO assignments of the valence band for: poly(vinyl alcohol) based upon the XPS spectrum and MO assignments for water; polystyrene based upon the XPS spectrum and MO assignments for benzene; poly(vinyl cyclohexane) based upon the XPS spectrum and MO assignments for cyclohexane; poly(1-butene) based upon the XPS spectrum and MO assignments for n-butane; and polypropylene based upon the XPS spectrum and MO assignments of propane. The degree of correspondence appears to be good, even in the case of

comparison between poly(vinyl alcohol) and water, once the carbon peaks are taken into account. Salaneck⁵⁵ gained insight into the assignment of spectral features by comparison of XPS and UPS spectra for various compounds related to the polymer repeat unit structure. He compared the UPS spectrum of polystyrene with the XPS spectra of polystyrene and benzene, and with the UPS spectra of ethyl benzene and benzene. He also performed this type of comparison for poly(2-vinyl pyridine), polyacetylene, and polypyrrole. This method permitted Salaneck to determine the contribution from the different structural units, and to determine the nature of the peaks.

The methods used by Pireaux, et al. and Salaneck for valence band assignments were also used in the present work to assign valence peaks for the SDS system. The particular assignments will be discussed in the Results and Discussion chapter, but were made from model compounds with similar chemical features as the various repeat units involved, benzene for PS and trans-2-butene for PB and PI.

3.3.3 QUANTIFICATION OF THE VALENCE BAND

In order to perform a quantitative or semi-quantitative analysis of the valence band the spectra must first be modified. The modifications necessary are baseline subtraction to remove the background noise and inelastic (loss)

photoelectrons, and energy referencing to insure that all the spectra compared are correctly aligned.

Baseline subtraction was performed by non-linear subtraction which is generally accepted as the more accurate method of baseline subtraction. For most core peaks the background noise is rather uniform immediately prior to and following the peak. Consequently, the difference between linear and non-linear baseline subtraction is very small. However, in the valence band the background noise varies from a high level prior to the peaks, to zero after the peak (beyond 0 eV). The background prior to the peaks is generally 20% to 50% of the pre-subtraction peak intensity. Consequently, in the valence band the method of baseline subtraction will greatly affect the relative peak heights, and non-linear subtraction must be used. The effect of the method of baseline subtraction on the valence band appearance is shown in Figure 7.

Non-linear baseline subtraction is the subtraction of a fraction of the difference in background noise on either side of the peak which is proportional to the enveloped peak area at each specific energy. this can be expressed mathematically as:

$$I_{\text{true}} = I_{\text{exp}} - \delta * \frac{\int_{E_{\text{init}}}^E I(E) dE}{\int_{E_{\text{init}}}^{E_{\text{final}}} I(E) dE}$$

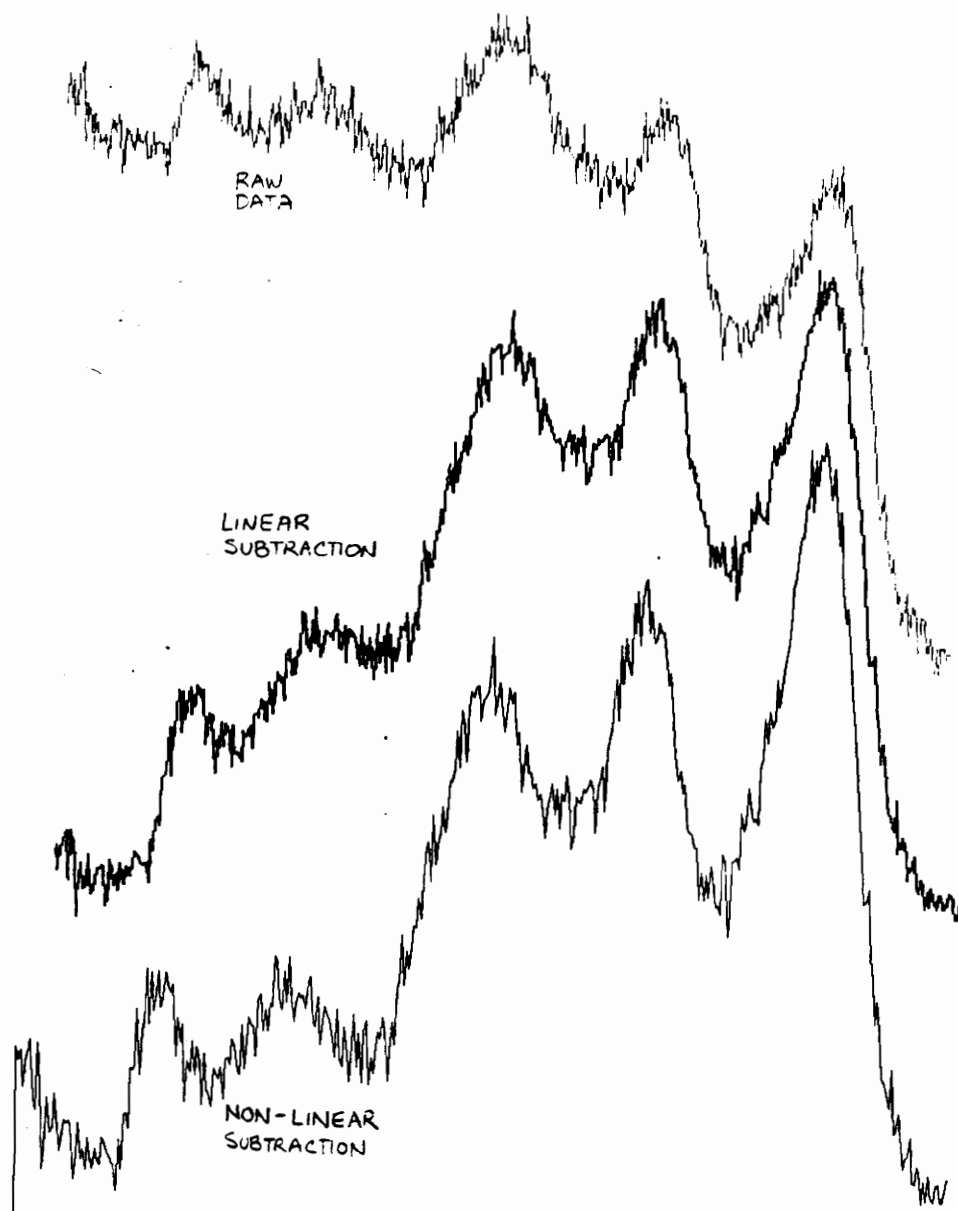


Figure 7. Effect of Method of Baseline Subtraction

Where I =intensity of the true data or the experimental data, E =binding energy in eV, and δ =the difference in background noise levels before and after the peak. The physical basis is that the amount of background is determined by inelastic collisions of photoelectrons as they try to leave the sample. Hence, the number of electrons suffering inelastic collisions, (inelastic collisions cause loss of kinetic energy), at a particular kinetic energy point is proportional to the number of no-loss electrons at all higher kinetic energies. This is the basis of computer code written to subtract the baseline, which is included as Appendix A. Due to the fact that each time the baseline is calculated the valence band shape changes, the computer program iterated until the rms (root mean square) difference between two consecutive baseline calculations was less than 0.5%. This method of baseline subtraction is essentially identical to that used by Pireaux, et al.⁵⁴ .

Energy referencing was performed by setting the Cls peak center to 285.0 eV and applying the corresponding charge correction to the valence band. As noted by Pireaux, et al.⁵⁴ the chemical shift of the Cls peak for different polymers is different, consequently referencing to 285.0 eV for all polymers is not equally valid. However, they noted that the chemical shift for the Cls peak of polymers such as polystyrene, polypropylene, poly(vinyl cyclohexane), and poly(1-butene) all lie within 0.5 eV of one another. Major

chemical shift differences of 4 to 5 eV are only observed between the polymers listed and halogenated or other very polar polymers. Salaneck⁵⁵, as mentioned above, quantified the amount of cis and trans in a polyacetylene sample. During this study he investigated the effects of energy referencing errors and found that a shift of 0.5 eV in either direction had no effect on the quantification results. Therefore, the energy referencing based on 285.0 eV for Cls is valid for the SDS system results since polystyrene, polybutadiene, and polyisoprene have small Cls chemical shift differences between them.

The principal technique used to quantify the valence band was to measure valence band intensities at several binding energies. These binding energies were determined by the energies of peaks on the homopolymer scans. In most cases these peaks were correlated to specific molecular orbitals. A computer procedure to add weighted amounts of the homopolymer peaks to obtain a close fit to the experimental data gave poor results. This was attributed to the unresolved nature of the valence band, as well as a specific orientation of the polymer repeat units at the surface. This orientation caused the valence band spectra to change in shape at different exit angles.

4.0 EXPERIMENTAL

The following sections cover the materials and methods used in this study for the two polymer systems studied.

4.1 MATERIALS

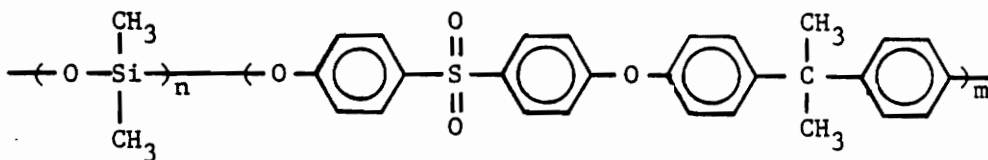
The polymers examined during this study were separated into two systems: polysiloxane-polysulfone [PDMS-PSF]; and polystyrene-polydiene [PS-PD].

The poly(dimethyl siloxane-b-bisphenol A sulfone), [PDMS-b-SF], multiblock copolymer was obtained from Professor J. E. McGrath's polymer synthesis laboratory at Virginia Tech. The polysulfone, [PSF], is the commercial polymer Udel supplied by Union Carbide Corporation. Figure 8 shows the characterization data and structures of the polymers studied in this system.

Two types of diene components, and one type of polystyrene were studied. The block copolymers were triblock poly(styrene-butadiene-styrene), [SBS], and poly(styrene-isoprene-styrene), [SIS]. The diene homopolymers used were polybutadiene [PB], and polyisoprene [PI]. All of these polymers were purchased from Scientific Polymer Products, Inc. of Ontario, New York. The polystyrene [PS] was supplied by the Dow Chemical Company. Figure 9 shows the structures

Block Copolymer:

Poly(dimethyl siloxane-b-bisphenol A sulfone)



Siloxane block length = 4919 gr/mole

Sulfone block length = 11638 gr/mole

Intrinsic viscosity in chloroform at 25°C = 0.67 dl/gr

Homopolymer:

Poly(bisphenol A sulfone)

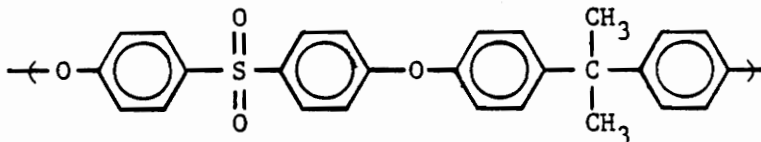
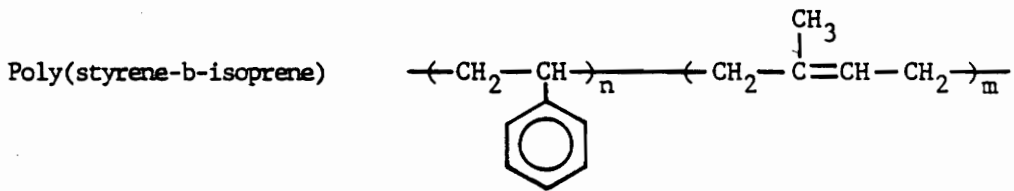
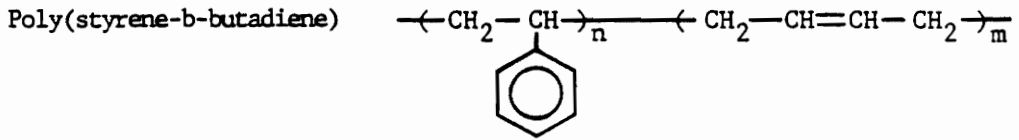


Figure 8. Structure and Characterization of PDMS-PSE System

Block Copolymers:



Homopolymers:

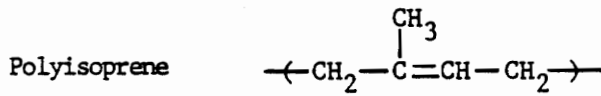
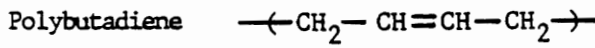
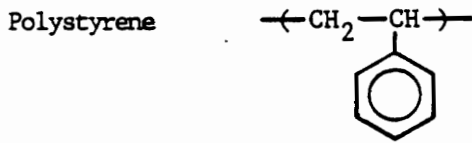


Figure 9. Structure of PS-PD System

Polymer	PS %	Molecular Weight Distribution*			PD %cis
		M_n (x1000)	M_w (x1000)	M_z (x1000)	
SBS	30	124.5	161.1	--	Unknown
SIS	14	92.0	141.5	--	Unknown
PS-1	100	77.8	196.0	346.0	--
PS-2	100	117.0	295.0	489.0	--
PS-3	100	45.6	211.0	405.0	--
cis-PB	0	200-300	--	--	98
cis-PI	0	--	--	--	Unknown

* Size Exclusion Chromatography courtesy of Professor T. C. Ward's polymer characterization laboratory.

Figure 10. Characterization of PS-PD System

and Figure 10 shows the characterization data of the polymers in this system. The size exclusion chromatography (SEC) to determine the molecular weight distribution of the SBS and SIS copolymers was performed in Professor T. C. Ward's polymer characterization laboratory. The block copolymer molecular weights are shown in units of the molecular weight of polystyrene with identical elution characteristics. If one assumes that the styrene blocks elute identically to polystyrene homopolymer (as did McIntyre and Campos-Lopez⁸), then the molecular weight can be broken down to block weights. Hence, the block number average molecular weights are 13,800-64,400-13,800 for SBS and 17,400-107,100-17,400 for SIS. Note that the numerical value for the center diene block is still in units of molecular weight of polystyrene with identical elution properties.

4.2 METHODS

Angular dependent XPS was used to determine the chemical concentration profile in the sample films. This method, as described in the previous section, enabled the determination of the concentration profile in the top 6 nm of the surface. The angle was varied by rotation of the sample probe, thus varying the angle between the sample surface plane and the electron energy analyzer axis. Angles of 90°, 30°, and 10° were used, with 10° being the grazing angle with the smallest

depth of analysis. The XPS instrument used in this study was the Kratos XSAM 800. All of the spectra were collected using the magnesium x-ray source (photon energy of 1253.6 eV) operating at 13kV potential and 20mA emission current. The vacuum during spectra collection ranged from 10^{-9} to 10^{-7} torr. Even though the pressure was relatively high in some cases, no evidence of solvent in the spectra could be detected. (This was determined by looking for chlorine peaks for chloroform cast films, and by comparing the carbon and oxygen peaks for toluene and THF cast films.)

XPS data processing was performed using standard as well as some new techniques. For the PDMS-PSF system only core level peaks were collected and standard data processing techniques were used to convert peak area ratios into atomic percentages. For the PS-PD system, on the other hand, both core and valence level peaks were collected. The core level peaks collected were the Cls and its shakeup peak. The valence level data processing was described in the Valence Band Quantification section. In all of the samples analyzed for both systems the correction for sample charging was performed by assigning the Cls peak to 285.0 eV.

All of the samples studied were solvent cast films. To establish the effects of kinetics on the surface, the rate of solvent evaporation was varied by a crude control of the atmosphere over the solution. The higher the solvent concentration above the solution the longer the time to form a

film, and the longer the surface region was plasticized by the solvent. In the plasticized state rearrangements at the surface could more readily occur. Hence, the longer the time to form a film the longer the surface region had for polymer rearrangements.

Several types of sample preparation were used to cast the films in the PDMS-PSF system. Films were cast from 1:20 solutions of chloroform (1 gram of polymer to 20 cc of chloroform) in glass petri dishes to form films about 2mm thick. The cover of the petri dish was removed to achieve a fast evaporation rate (the film was formed in about 3.25 hours). The cover was placed over the petri dish to achieve a slow evaporation rate (the film was formed in about 80 hours). The films for studies of the effects of substrate were cast from 1:20 chloroform solutions on water and were formed in 1 to 3 minutes. These films were very thin, of the order of 100nm. The films cast on mercury were very much thicker, (about 2mm) and were formed in about 80 hours. Mercury, like most metals, oxidizes quickly upon exposure to atmospheric oxygen. To avoid casting on an oxide surface, mercury was drawn up with a syringe from the center of the liquid mass (the oxide slag is on the surface of the liquid mass) and expelled beneath the surface of the solution, thus avoiding direct contact with atmospheric oxygen.

Two methods of sample preparation were used to prepare films in the PS-PD system. Films were cast from 1:20 sol-

utions of either toluene or tetrahydrofuran (THF). Films were cast in glass petri dishes to form films about 2mm thick. The film formation from toluene with the cover removed took 7 days, and with the cover in place took 28 days. The evaporation of THF with the cover removed took 4 days and with the cover in place took about 14 days. Films were also cast from THF using a special procedure which produced a very rapid rate of solvent evaporation. A strip of clean aluminum foil was dipped in a 1:10 polymer solution and slowly withdrawn. The resulting polymer films were air dried and then vacuum dried in the XPS sample introduction chamber. The entire film formation took from 5 to 10 minutes.

5.0 RESULTS AND DISCUSSION

This chapter contains two sections devoted to the two polymer systems studied, PDMS-PSF and PS-PD. The PS-PD section is further divided into a subsection covering the shake-up peak analysis and a subsection covering the valence band analysis.

5.1 POLY(DIMETHYL SILOXANE-B-SULFONE) SYSTEM

The ESCA wide scan spectra of the component homopolymers are shown in Figure 11. As can be seen by comparing the spectra both PDMS and PSF repeat units give rise to carbon C1s and oxygen O1s peaks. However, each repeat unit also has an unique heteroatom, which gives two additional sets of intense peaks useful to monitor composition. PSF contains sulfur which gives rise to the S2s and S2p peaks, and PDMS contains silicon which gives rise to the Si2s and Si2p peaks.

This work required the determination of repeat unit weight percentages, hence ratios of two spectral peaks were made and equations were developed to convert the area ratio into weight percent of siloxane repeat units. These calculations were performed in a manner similar to that presented by N. Patel^{5,6}. The equations used to determine weight percent siloxane repeat units from core peak area ratios are

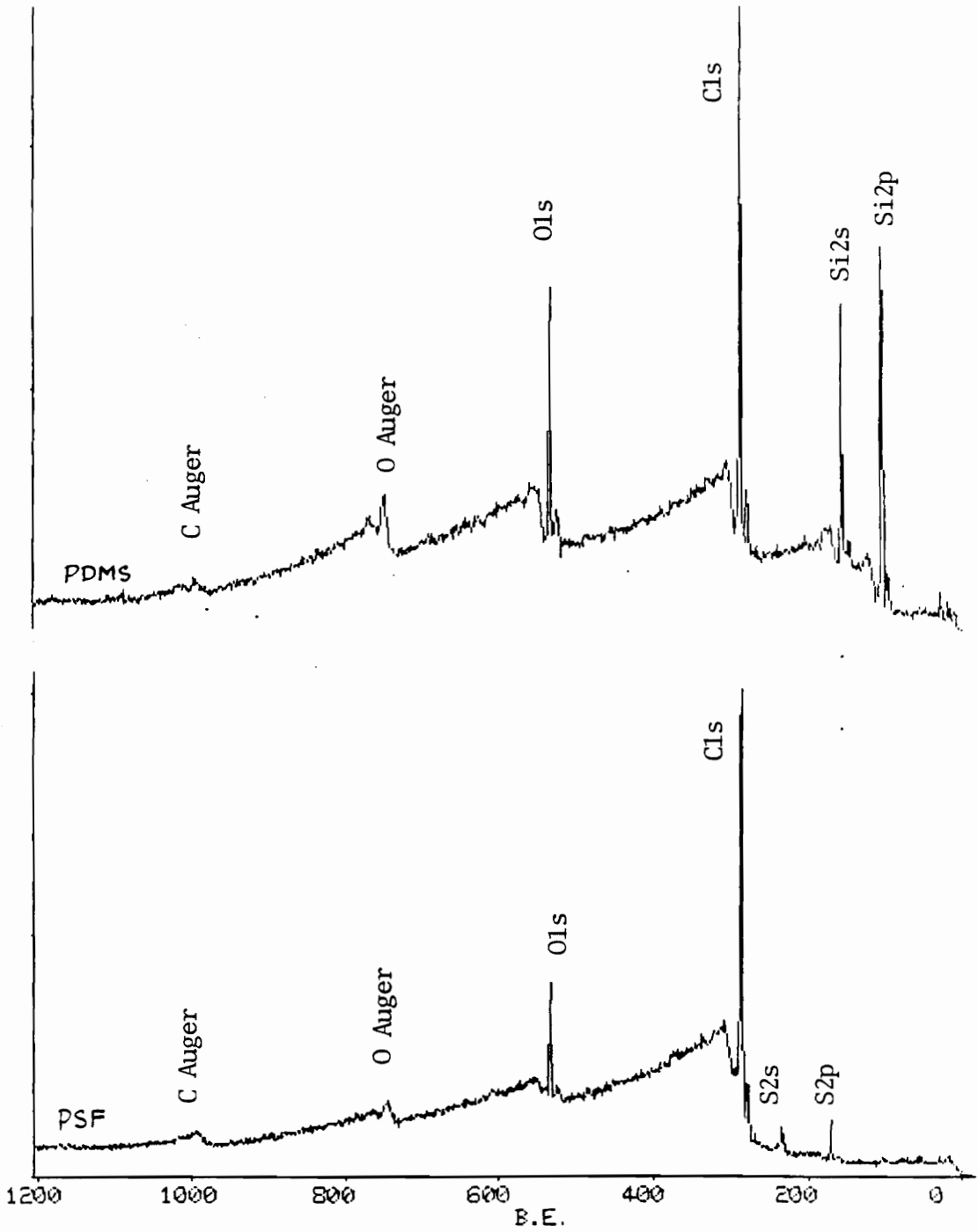


Figure 11. Wide Scan Spectra of PDMS and PSF.

$$\text{Weight \% Siloxane} = 100\% * \frac{1}{1 + 2.9943 * (S/Si)}$$

Where: (S/Si) = S2p to Si2s area ratio

$$\text{Weight \% Siloxane} = 100\% * \frac{1}{1 + 3.5536 * (S/Si)}$$

Where: (S/Si) = S2p to Si2p area ratio, (using
the experimentally corrected
SPC for Si2p)

Figure 12. Siloxane Concentration Quantification Equations

shown in Figure 12. The detailed development of both equations is given in Appendix B. During the initial stages of the present work equations were developed to use ratios based on the C1s, O1s, S2p, and Si2p peaks. However, in some cases the results did not check with each other, this is probably due to slight hydrocarbon contamination or surface oxidation. In order to remove the effects of possible hydrocarbon contamination and surface oxidation, the sulfur and silicon peaks were chosen for the ratio. Initially the S2p and Si2p were chosen to monitor the concentration due to these peaks being the most intense from each heteroatom. However, after running several spectra on PDMS standards it became evident that the literature value for the cross-section of Si2p (20.7 kilobarns) was inconsistent with data collected in the present study. As a consequence a new value was experimentally determined (21.1 kilobarns) by forcing equally based on stoichiometry between the C1s, O1s, Si2p, and Si2s for PDMS. That value was then used to modify all the data collected up until that point. But from that point on, the S2p and Si2s peaks were used to determine the concentration data. The values of those peak cross-sections were found to be consistent with my data. The S2p and Si2s peaks also had the advantage of being nearly the same binding energy. This enabled the collection of the sulfur to silicon ratio at essentially the same depth into the sample, (analyzing depth is a function of photoelectron energy). Due to

the weak signal from the S2p, any siloxane weight percent above 90% is prone to area measurement errors and is essentially indistinguishable, experimentally, from 100% siloxane. (The weak signal arises from the low sulfur content per repeat unit weight (1:442) as compared with the high silicon content per repeat unit weight (1:74).) For the remaining siloxane concentration range the error was estimated to be 5 to 10%. Note that only the concentration profiles on the mercury and water cast films were determined from the S2p to Si2s peak ratios.

5.1.1 CONCENTRATION PROFILE VERSUS EVAPORATION RATE

Surface concentration profile studies were conducted on blends of 1% by weight block copolymer in PSF at two rates of chloroform evaporation. The slow rate of evaporation cast films from 1:20 chloroform solutions in approximately 80 hours, (4800 minutes). The fast rate of evaporation cast a film from an identical solution in about 3.25 hours, (200 minutes). The evaporation rates are approximate due to the crude control of the atmosphere over the film which consisted of having the petri dish cover either in place or removed. Nevertheless, the slow evaporation rate film took about 25 times longer to form than the fast evaporation rate film. The surface concentration profiles resulting from the two evaporation rates for a 1% by weight blend of block copolymer

in PSF is shown in Figure 13. For comparison the profile found by N. Patel⁵⁶ on a similar polymer blend for a very fast evaporation is also shown. N. Patel's films were cast from chloroform solutions of similar concentrations as those in the present work, but the film was about 0.5mm thick. As a consequence of the thickness difference, Patel's film was formed about 10 to 20 times faster (10 to 20 minutes) than the fast evaporation rate films made during the present study.

Examination of the curves shows a distinct trend in the concentration profiles versus evaporation rate. As the evaporation rate increases the gradient steepens and the surface concentration decreases slightly. This behavior can be readily rationalized on the basis that the slower evaporation rates permits a closer approach to equilibrium conditions of surface energy driven siloxane surface segregation, and siloxane-sulfone phase separation. At faster evaporation rates the surface energy driving force still causes a strong surface segregation of siloxane, but the phase separation deeper into the bulk is incomplete when the polymer mobility decreases to the low solid state value due to solvent evaporation. At slower evaporation rates both more complete surface segregation and more complete phase separation can occur. Consequently, it seems that the longer the polymer chains are highly mobile (in the solvated or plasticized state) the higher the degree of siloxane segregation to the

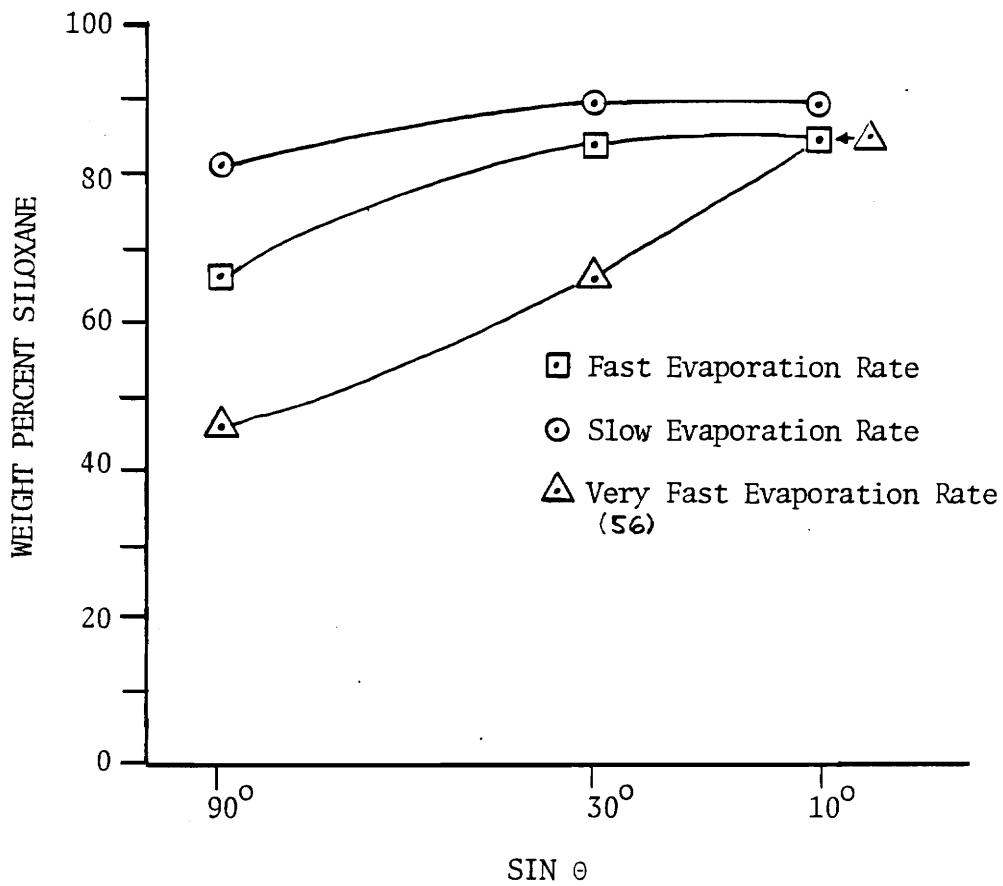


Figure 13. Siloxane Concentration Profile for Various Evaporation Rate.

surface, and phase separation deeper into the bulk. Even at the fast evaporation rate used in the present study, and the faster rate used by N. Patel, the surface had a very high concentration of siloxane due to the tremendous surface energy driving force in this system.

5.1.2 CONCENTRATION PROFILE VERSUS SOLVENT

Although no work was performed during the present study along this line of investigation for the PSF-PDMS system, literature data does provide additional insight into the surface segregation of siloxane block copolymers. Work by Clark, et al.⁴⁹ on poly(styrene-b-dimethylsiloxane) diblocks containing 41% by weight siloxane showed variations in the surface composition with films cast from different solvents. Their surface analysis consisted of XPS at normal (90°) takeoff angle. Using the assumption of a uniform overlayer of siloxane repeat units over the copolymer, they then calculated the corresponding thickness of the siloxane overlayer. Although they offered no reason for using the uniform overlayer model of surface segregation, the use of this model is consistent with the observed trends in the present work. That is, the concentration of siloxane at the surface is only slightly affected by film formation characteristics, but the concentration profile deeper into the bulk (or overlayer thickness) varies greatly. From their data the solvents they

used could be put into one of two groups according to the calculated siloxane overlayer thickness. A 1.3 nm overlayer was calculated for films cast from cyclohexane, benzene, toluene, and chloroform. A 4.0 nm or greater overlayer was calculated for films cast from styrene and bromobenzene. Although they presented no explanation of this behavior, the two groups of solvents are separated by solubility parameter and vapor pressure (which is related to the evaporation rate).

The solubility parameters of the solvents in the first group of solvents range from 8.2 to 9.3 (cal/cc)**1/2, while those of the second group range from 9.3 to 9.9. The second group of solvents, therefore, are closer to polystyrene in solubility parameter than polydimethylsiloxane, and visa versa for the first group. The fact that the unfavorable solvents for PDMS produced a greater siloxane surface segregation can be envisioned to result from the addition of two driving forces. The first driving force is the decrease in surface free energy resulting from siloxane surface segregation. The second driving force is the incompatibility between the solvent and siloxane which forces the siloxane away from the bulk (rich in solvent) to the surface as the film is being formed.

The first group of solvents also have vapor pressures at 25°C from 4 to 37 times those of the second group. Consequently, the films cast from solvents in the first group were

formed quicker and had less time to equilibrate than those cast from solvents in the second group. This has been shown to reduce the siloxane surface concentration and increase the concentration gradient at the surface in the PDMS-PSF system, as noted in the preceding section. However, two solvents had the same solubility parameter yet different vapor pressures, and another two solvents had vapor pressures within a factor of 4 of each other yet different solubility parameters. Yet all of these various solvents produced one of only two overlayer thicknesses. Consequently, it appears that the overlayer thickness is affected by the solvent-polymer solubility parameter mismatch as well as the evaporation rate of the solvent.

5.1.3 CONCENTRATION PROFILE VERSUS CASTING SUBSTRATE

Blends of PDMS-b-PSF copolymer in PSF were cast on several substrates and surface concentration profile measurements were made on the air surface, as well as interfaces with two substrates. In order to eliminate artifacts caused by tearing and surface roughness caused by peeling a sample from a solid substrate, only fluid substrates were used. Mercury was chosen to represent a typical metal substrate, and water was chosen to represent a non-metallic, polar (non-solvent) substrate. Blends of 1% by weight block

copolymer in PSF were cast on mercury, and blends of 1.38% by weight block copolymer (1% siloxane) were cast on water.

The concentration profile for 1% by weight block copolymer in PSF cast on clean mercury is shown in Figure 14. It is immediately obvious upon inspection of the figure that there is a large difference in the concentration profiles between the air surface and mercury interface. The siloxane concentrations are nearly the same at the air surface and the mercury interface, but the concentration gradients deeper into the bulk are significantly different. The steeper gradient for the mercury interface can be explained by the competition between two opposing driving forces. There is the decrease in interface energy driving force which causes the strong segregation of the much lower surface energy siloxane blocks, (evidently siloxane segregation minimizes the mercury/polymer interfacial free energy). But there is also an opposing driving force due to the polar interaction between the sulfone blocks and the liquid mercury. As a consequence of the interplay of the two competing forces there is a suppression of the concentration profile. The surface concentration and interface concentration are nearly the same due to the large difference in air surface energy and mercury interface energy between the siloxane and sulfone blocks. The gradient deeper into the polymer reflects the electronic environment produced by mercury which tends to increase the sulfone concentration.

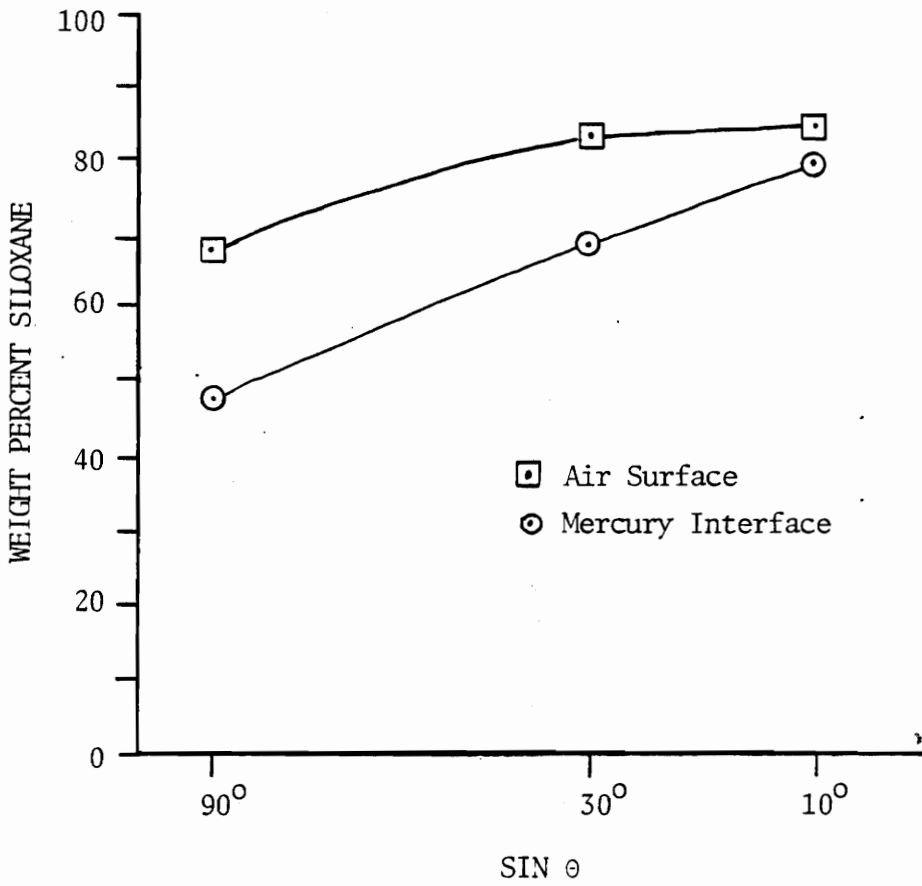


Figure 14. Siloxane Concentration Profile on Clean Mercury.

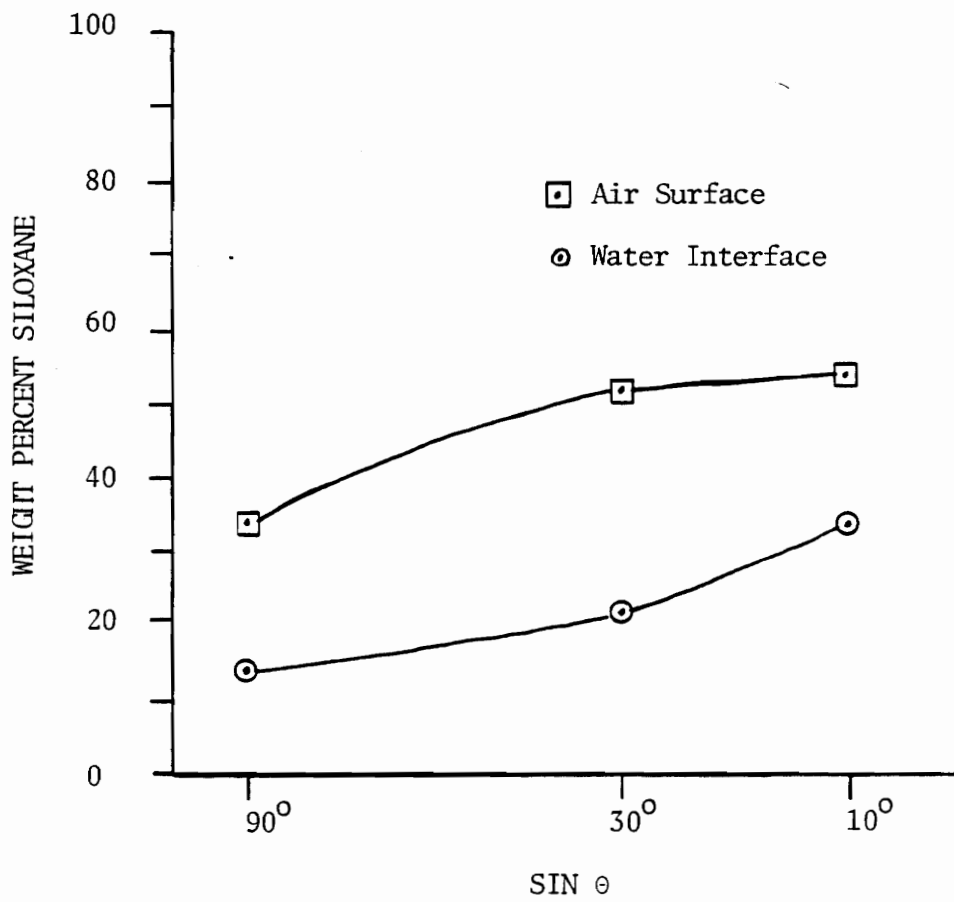


Figure 15. Siloxane Concentration Profile on Water.

The concentration profile for a blend of 1% by weight siloxane (1.38% by weight block copolymer) in PSF cast on a water interface is shown in Figure 15. In this case the air surface concentration is considerably higher than the water interface concentration, but the concentration gradients are similar. Investigation of other siloxane compositions from 72% to 0.1% all showed the same trend. In all cases the water side had a lower concentration of siloxane than the air side, and the concentration gradients of the two sides had similar slopes. However, the 1% siloxane case represented the largest variation in concentrations.

The fact that the air surface and water interface had concentration gradients with similar slopes indicates the absence of strong electronic interactions between the PDMS or PSF blocks and liquid water. This is reasonable since water does not have the same magnitude or type of electronic forces as mercury, (which had affected the concentration gradient).

The fact that the water cast film and the mercury cast film had significantly different concentration profiles may be attributed to sample preparation factors. The mercury film was formed at a slow rate while the water film was formed at an ultrafast rate. Consequently, the the film formation kinetics were vastly different and may have influenced the profile. The fact that the bulk composition was 1% copolymer for the mercury film and 1.38% copolymer for the water case

may also influence the profile. Solution-substrate interactions may also affect the concentration profile. The casting solvent may be attracted to or repelled from the interface depending upon the electronic and solubility characteristics of the solvent. the interfacial free energy of the solution against the substrate would also influence which solution component would segregate to the interface during film formation.

Another point which may cause the observed difference between the water and mercury films is the interfacial free energy characteristics of the substrates. The free energy at the mercury/polymer interface may be minimized by a different siloxane concentration than the water/polymer interface.

An experimental point of some concern initially was the time span between removing the film from the substrate and analyzing its concentration profile. The samples used were all processed away from the substrate, some for 4 or more hours before being analyzed. However, appreciable diffusion to alter the concentration profile did not occur. This was proven by E. A. Corragin⁵⁷ who cast a 100% PDMS-b-PSF copolymer film on a water substrate (the films were about 2mm thick). She found that after as much as 5 hours at 150°C there was no noticeable change in the concentration of siloxane (at normal analysis angle). A change was expected due to the difference in siloxane concentration between the

air side and the water side. However, the block copolymer chains were unable to diffuse due to the rigidity of the PSF blocks which, even at 150°C, were well below their glass transition temperature. Consequently, for PSF containing systems the length of time between separation from the substrate and analysis has no effect of the concentration profile. However, on systems where the times are longer, or temperatures are closer to the glass transition temperature the gradient may become affected prior to analysis.

5.1.4 GENERAL REMARKS

In all cases studied the PDMS-b-SF concentration profile appears to follow a pattern. The concentration at the outermost surface (10° analysis angle) is very slightly affected by the casting rate or the solvent. However, the surface concentration seems to depend upon the substrate. At deeper angles (90° and 30°) the concentration of siloxane varied significantly and depended upon the casting rate, substrate, and solvent. In general, the faster casting rates lead to a steeper concentration gradient, due to the lack of attainment of equilibrium before the PSF blocks become immobile. The more polar the substrate the steeper the concentration gradient as a result of the electronic interactions between the polar substrate and the polar PSF blocks. Data presented by Clark, et al. indicate that the lower the solvent-PDMS block

solubility the steeper the concentration gradient (or thinner the overlayer). However, in the PDMS-PSF system (and polystyrene-b-polydimethylsiloxane system studied by Clark, et al.) the huge difference in surface energy between the blocks resulted in a huge driving force for siloxane block surface segregation. Therefore, in all but one case investigated the concentration gradient varied much more greatly than the surface concentration. Only in the water cast films did the surface concentration vary and the concentration gradient remained the same. This is probably the result of specific surface properties not fully understood in the current literature.

5.2 POLY(STYRENE-DIENE-STYRENE) SYSTEM: SHAKE-UP ANALYSIS

The XPS wide scan spectra of the component homopolymers are shown in Figure 16. As can be seen by comparing the spectra PS, PB, and PI all give rise to Cls peaks, and very small O1s peaks, (due to surface oxidation). However, the narrow scans of the Cls core peaks show substantial variations in the Cls shake-up to main peak area ratio, as shown in Figure 17. As discussed previously all of the polymers contain pi-bonds and thereby give rise to a detectable shake-up peak. PS and PD have inherently different concentrations of pi-bonds as well as differences in the pi-bond electronic environment (aromatic versus aliphatic), hence

quantification based on the Cls main to shake-up area ratio is possible. As will be seen shortly there are several problems in converting the shake-up to main area ratio to an atom or repeat unit percentage. Consequently, the data are presented in the most direct format which is simply the ratio versus depth. The error in the ratio values were estimated to be about 10%.

5.2.1 ANALYSIS OF THE COMPONENT HOMOPOLYMERS

The shake-up to main ratios for the homopolymers were collected with the hope of being able to develop quantitative equations for PS content. The data collected for PB, PI, and PS are shown in Figure 18, Figure 19, and Figure 20, respectively. As can be seen on the figures the ratio is by no means constant with depth in the neat homopolymers. This could be caused by residual solvent, hydrocarbon contamination, or a variation in the probability of shake-up (valence co-photoionization) relative to the main photoionization process with depth. Comparing the THF versus toluene curves proves that the variation exists in both cases, hence residual solvent, if any, is not significant enough to cause this variation. There was a wide variety of sample preparation techniques used, with some films formed in minutes and others formed in weeks, however no differences in hydrocarbon or oxidation contamination were observed among

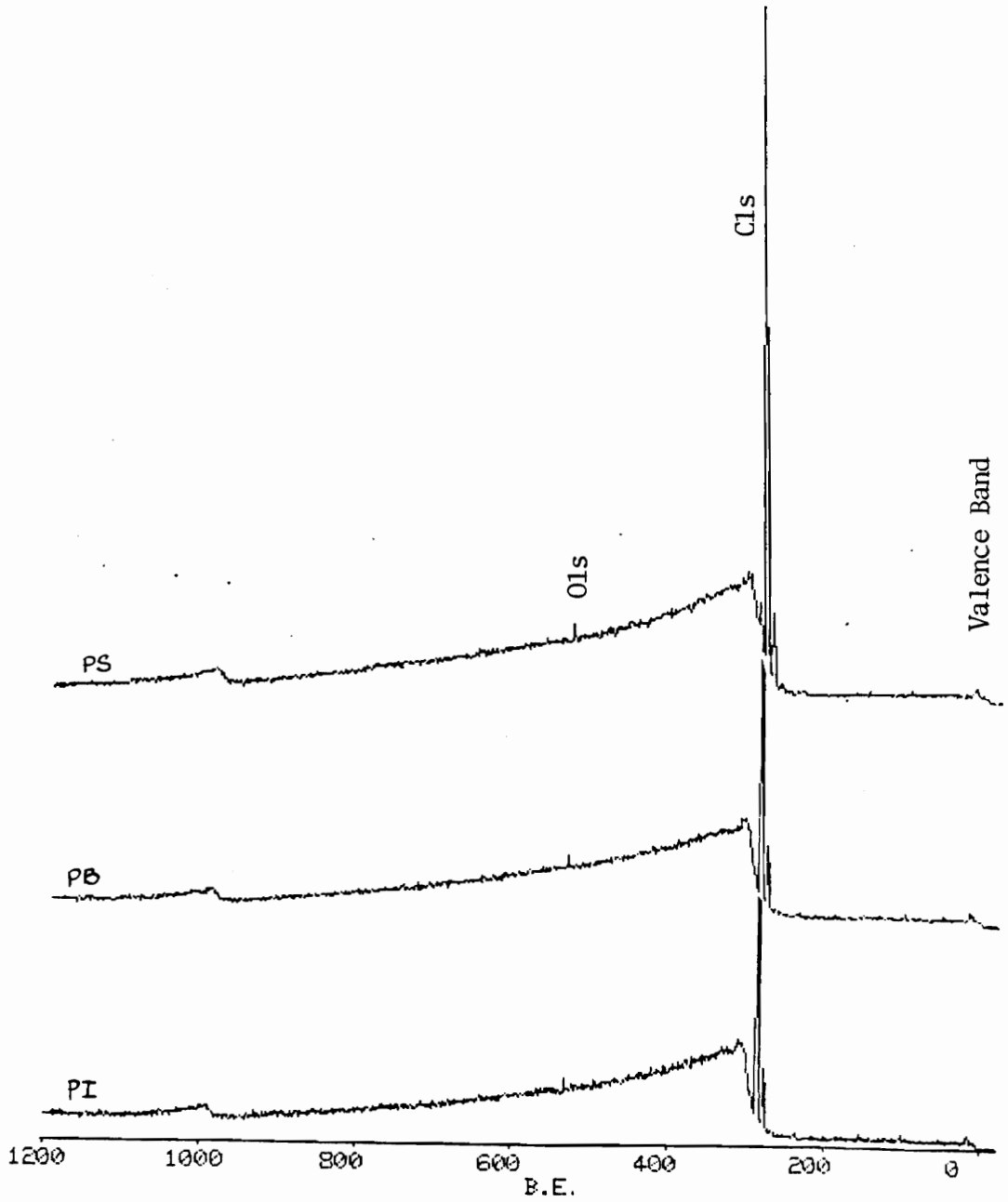


Figure 16. Wide Scans of PS, PB, and PI

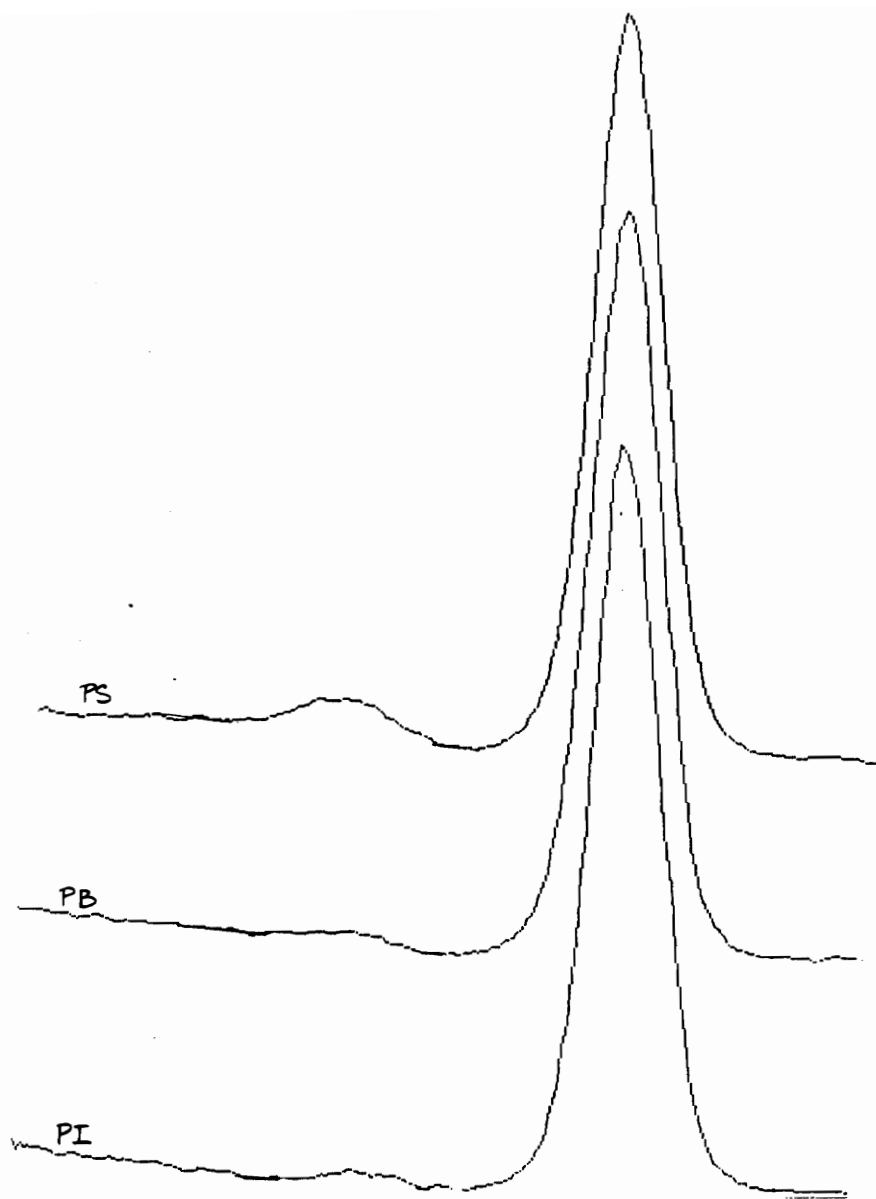


Figure 17. C1s Narrow Scans of PS, PB, and PI

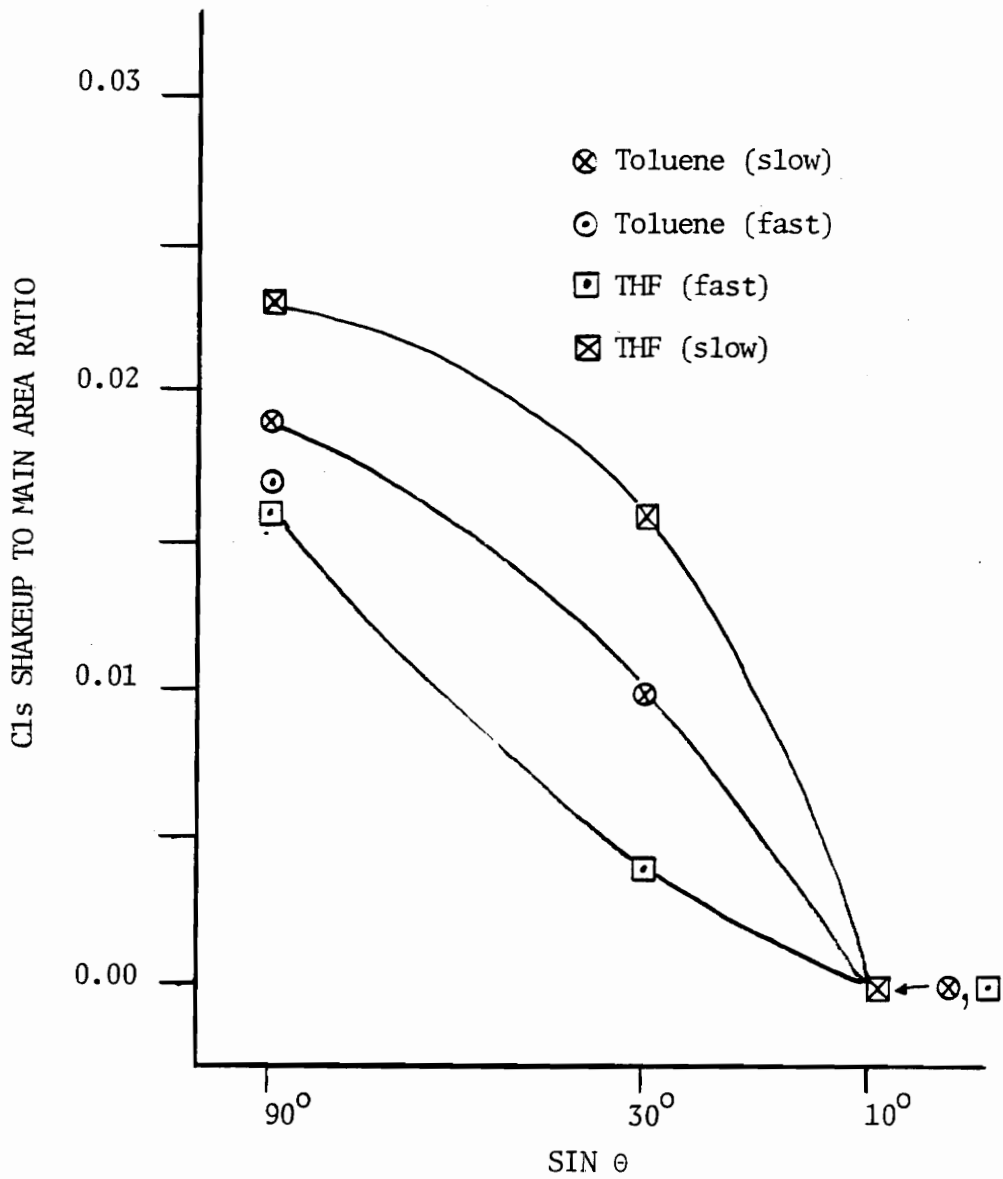


Figure 18. Shake-up To Main Ratio Versus Depth for Polybutadiene

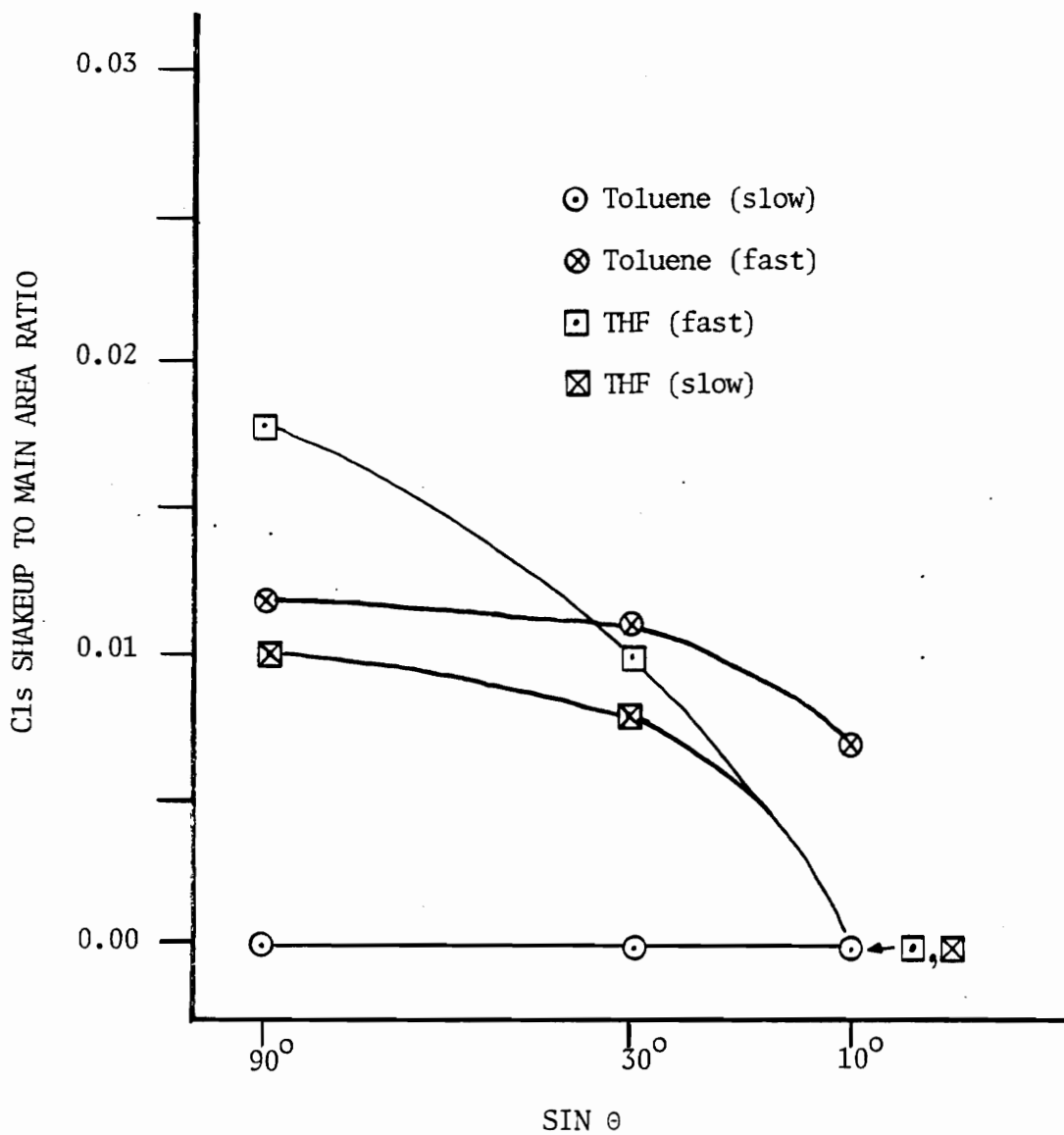


Figure 19. Shake-up To Main Ratio Versus Depth for Polyisoprene

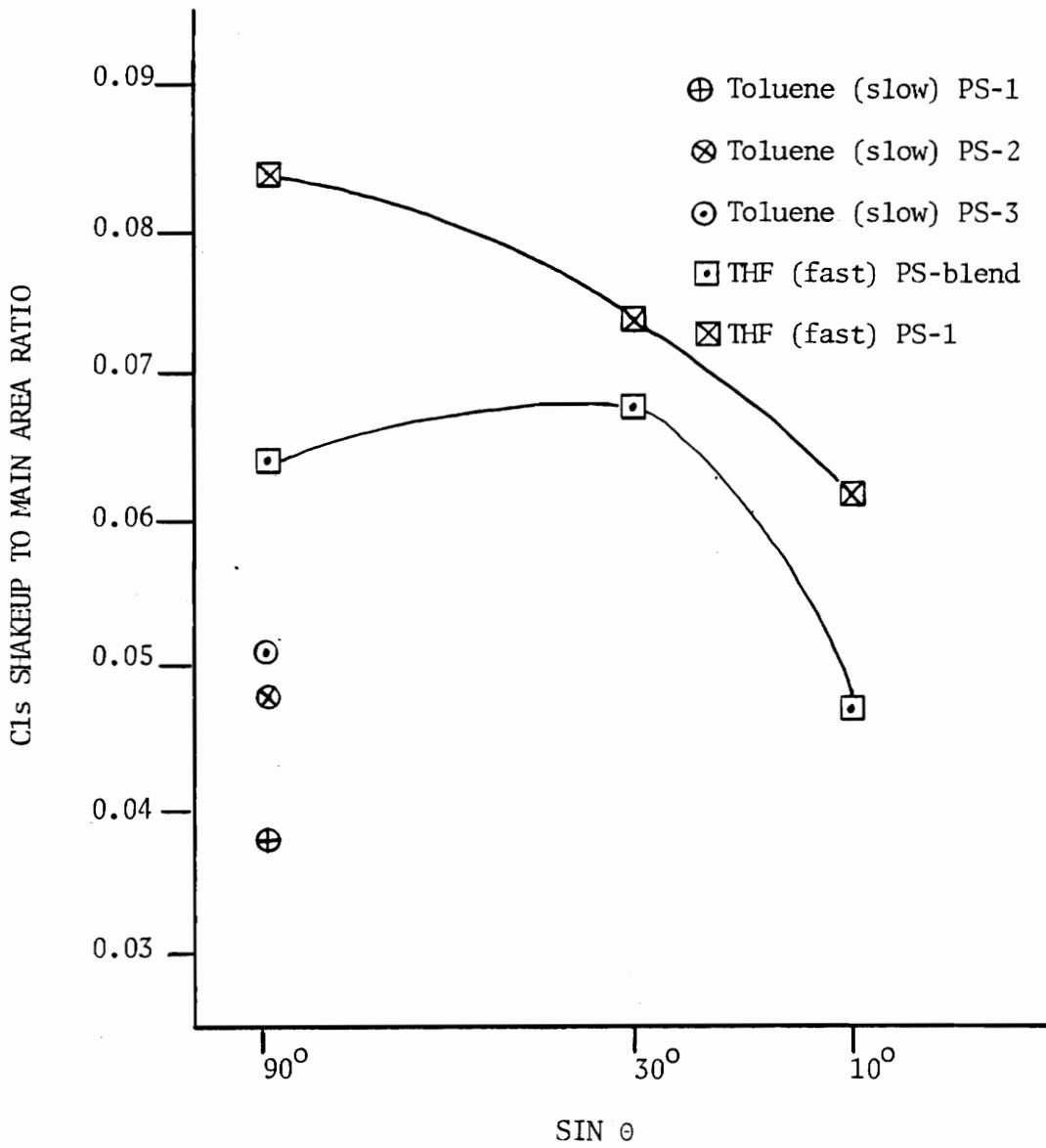


Figure 20. Shake-up To Main Ratio Versus Depth for Polystyrene

the films. In order to better understand the observed variation a study of the valence band was necessary. The valence band results will be discussed in a subsequent section, however, some of its results will be used here. It will be found that the observed variation is the result of orientation of the polymer repeat units at the surface. In the PI and PB cases the pi-bonds are oriented away from the surface. Although it will not be covered, a similar argument may hold for PS (the aromatic ring may be oriented away from the surface). The net effect of this orientation is an increase in pi-bond concentration with depth and thus a depletion at grazing angles, thus giving rise to the observed trends.

As a result of the orientation it is impossible to quantitatively measure the styrene concentration versus depth, and only qualitative statements can be made about the surface concentration profiles. The plots will be made for shake-up to main ratio versus depth (angle). The greater the shake-up to main ratio the higher the pi-bond concentration.

5.2.2 CONCENTRATION PROFILE VERSUS EVAPORATION RATE

Surface concentration profiles were measured on SBS and SIS block copolymer films cast from toluene at two different rates of evaporation. The films were cast from a 1:20 solution in glass petri dishes which either had the cover in place or removed. The evaporation with the cover in place

took 4 times as long as with the cover removed, (28 days versus 7 days). The concentration profiles for SBS are shown in Figure 21, and for SIS are shown in Figure 22.

Both sets of profiles show similar behavior with respect to surface segregation and the effects of evaporation rate. From inspection of the surface concentrations and concentration gradients it is clear that isoprene and butadiene blocks surface segregate. This is reasonable since the diene block has a slightly lower surface energy than the styrene block. Also, for the most part, the concentration profiles for the slow evaporation rate have a lower concentration of pi-bonds at all angles than the faster rate of evaporation. This is also reasonable since the longer the evaporation the closer the approach to equilibrium. In addition, in all cases the values of shake-up to main ratio is much lower than PS values and rather close to PD values.

5.2.3 CONCENTRATION PROFILE VERSUS SOLVENT

Surface concentration profiles were determined on both SBS and SIS block copolymers cast from toluene and THF. The profiles for SBS are shown in Figure 23 and for SIS are shown in Figure 24.

The effects of the solvent can be seen by comparing the slow toluene curves (nearly equilibrium for toluene cast films) with those of the fast cast THF films (formed in min-

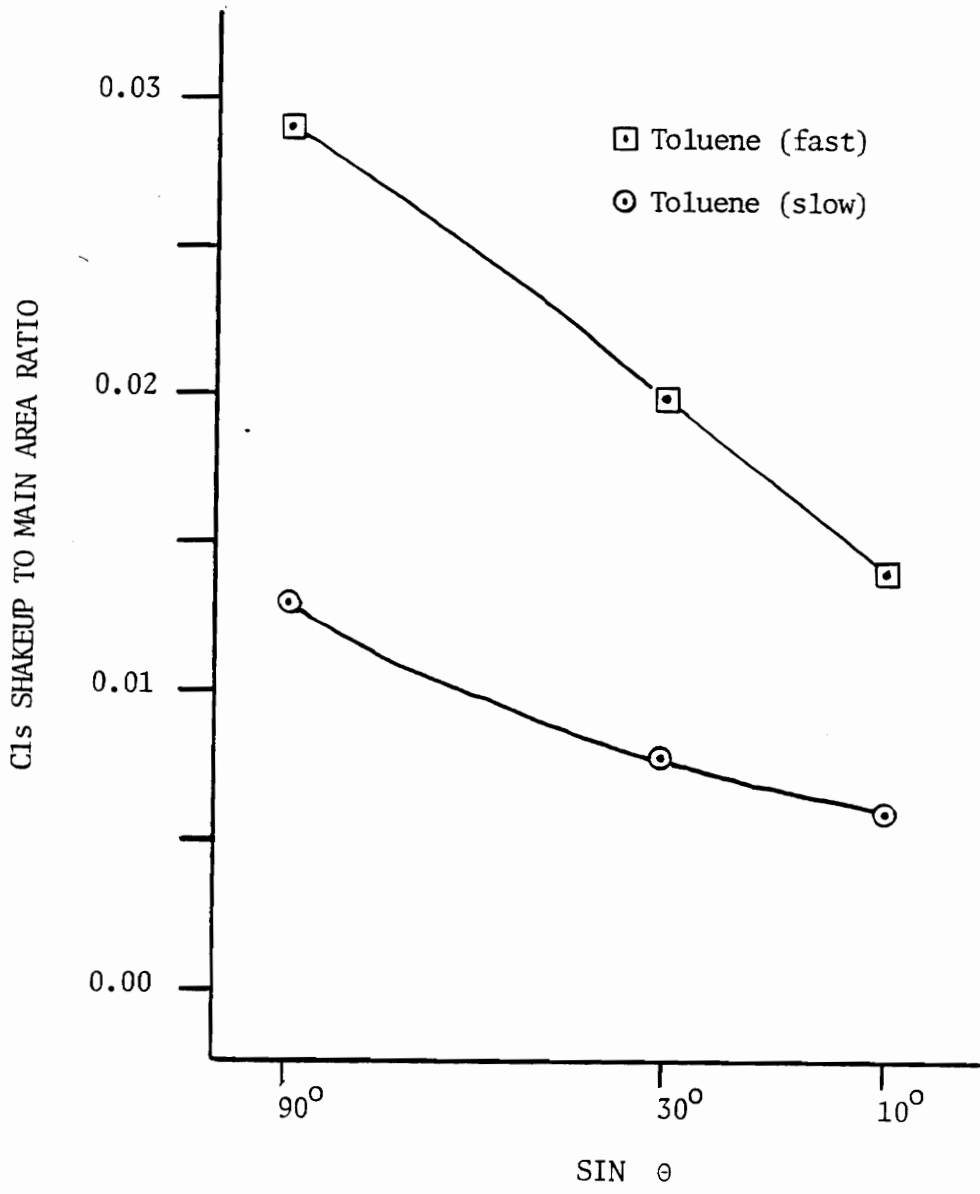


Figure 21. Concentration Profile for SBS Versus Rate of Evaporation

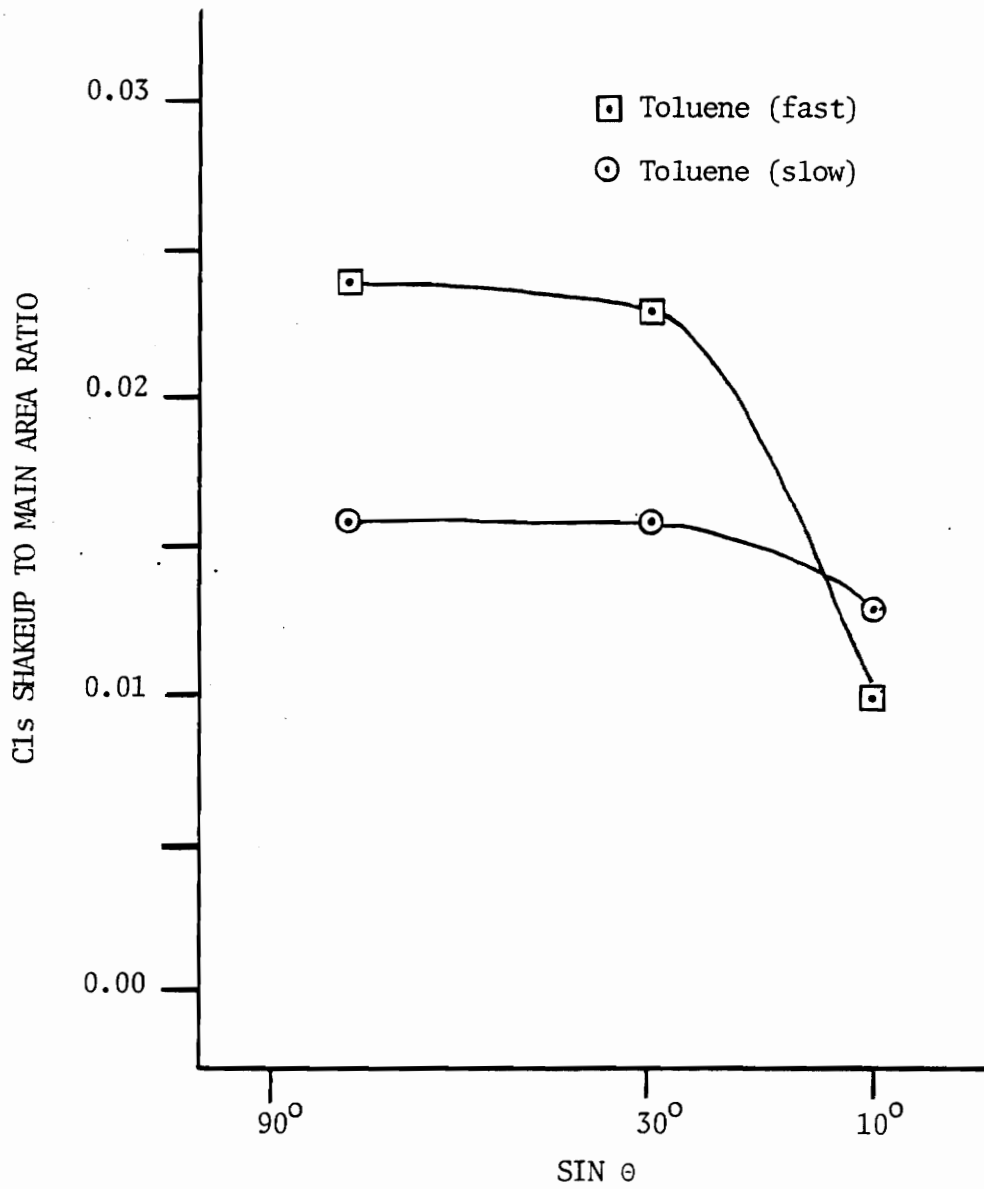


Figure 22. Concentration Profile for SIS Versus Rate of Evaporation

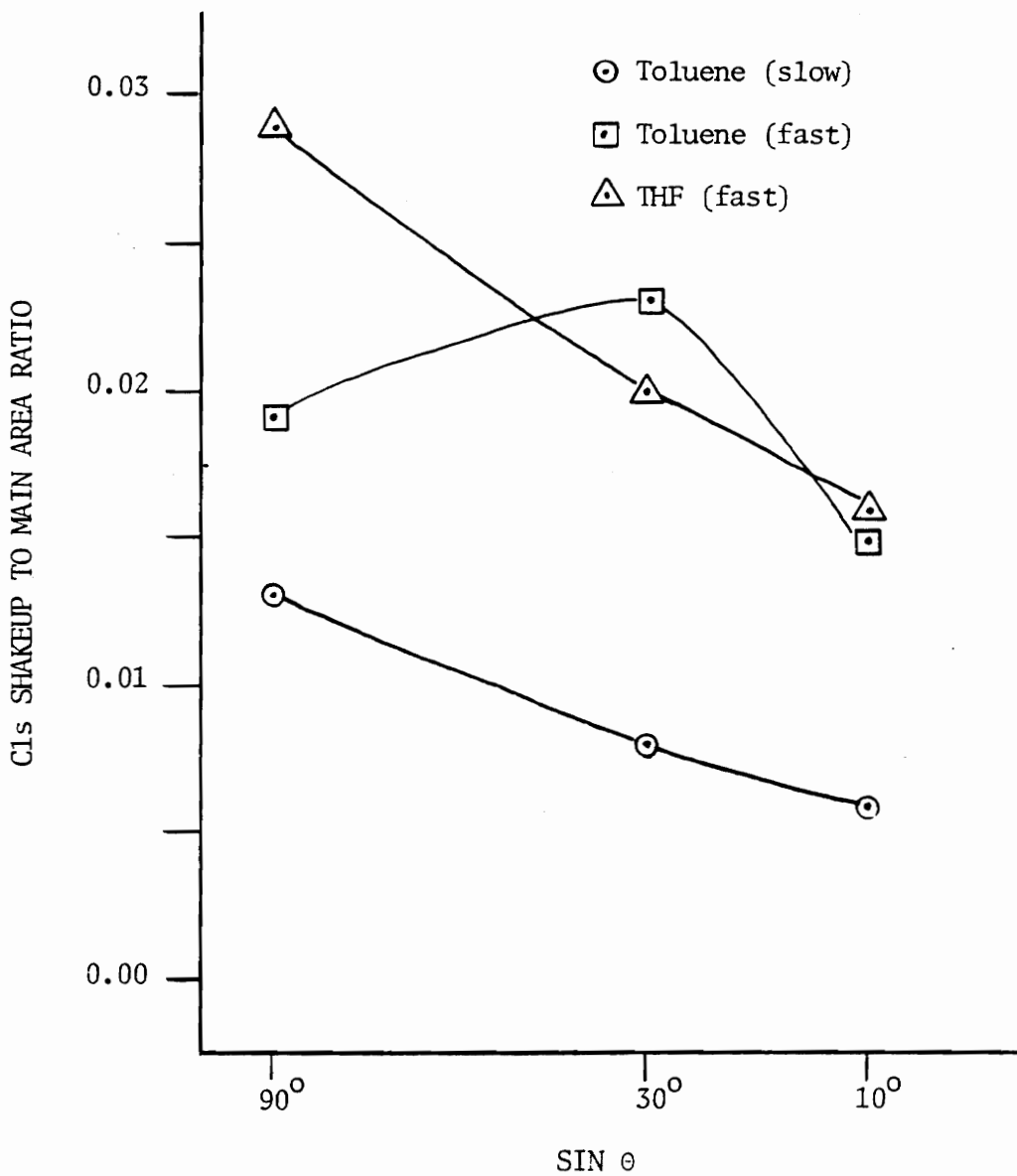


Figure 23. Concentration Profiles for SBS Versus Solvent

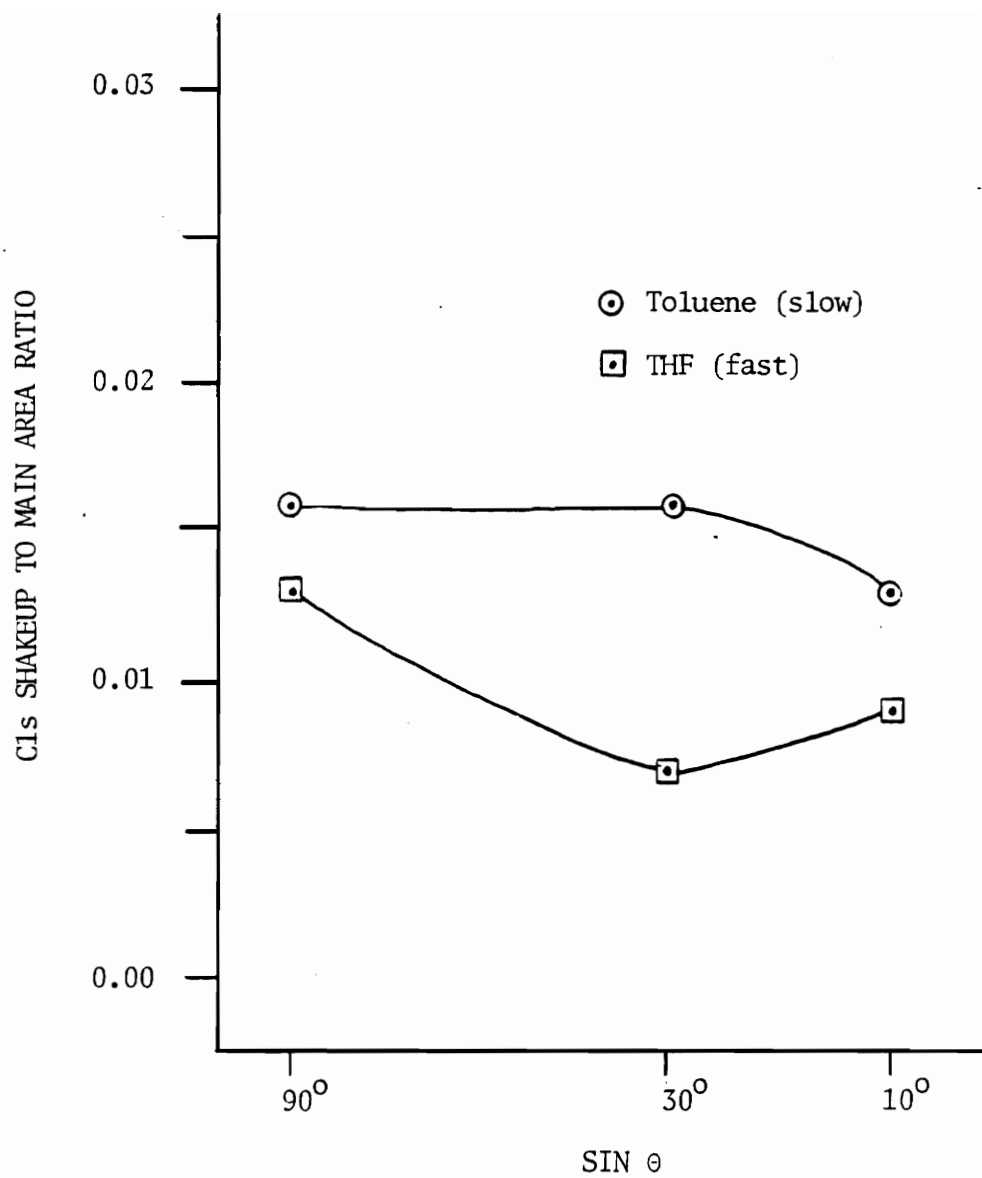


Figure 24. Concentration Profiles for SIS Versus Solvent

utes instead of days). For the SIS case, the THF cast film had a slightly more complete isoprene surface segregation than the toluene cast film even though the kinetics of the film formation would tend to indicate it should be higher in pi-bond concentration than the slow cast toluene film. For the SBS films the THF cast curve lies at a higher concentration than the slow toluene curve, however it lies near the fast cast toluene curve. Since the fast cast toluene film was formed in 7 days and the fast cast THF film was formed in only minutes, the close proximity of the curves indicates that either a kinetic limit in the gradient has been reached, or that there is an affect of the solvent on the gradient. Since the 90° concentration point is below that of the fast cast toluene curve, the indication is that the solvent is affecting the profile.

The fact that THF produces greater surface segregation than toluene for SIS can be rationalized on the basis of solubility parameters. The solubility parameter difference between THF and PI is larger than the difference between toluene and PI. Consequently, the isoprene blocks are expected to have a driving force causing surface segregation due to the lowering of the surface energy, as well as a lowering of the heat of mixing due to polymer - solvent incompatibility. This same argument holds for the butadiene blocks in SBS, but the incompatibility between PB and THF is less. Also, the PI blocks are estimated to be about twice

as long as the PB blocks, this will tend to make the PI blocks less soluble than PB blocks.

Both the SIS and SBS concentration profiles are much lower in pi-bond concentration than expected based on the very rapid rate of solvent evaporation. However, the slightly higher polymer-solvent incompatibility in the SIS case causes the concentration profile to lie even below the profile for the slow toluene film.

5.2.4 GENERAL REMARKS

The shake-up analysis of SBS and SIS cast at different evaporation rates and from different solvents shows reasonable trends. In all cases the diene block segregated to the film surface, which is reasonable because the diene block has a lower surface energy than the styrene block. The films formed at fast rates of solvent evaporation did not have as complete diene surface segregation or orientation due to the polymers becoming immobile before equilibrium was achieved. SIS films cast from THF showed much greater surface domination by the isoprene than the slowly cast toluene films. This is accounted for by the polymer - solvent incompatibility. This incompatibility is smaller in the SBS case, and consequently, the THF cast film had a concentration profile more influenced by the kinetics of film formation than by the polymer - solvent interactions. In summary, both the rate

of evaporation and the solvent (if it interacts strongly with the polymer blocks) have an effect on the surface concentration profile of SDS block copolymers, as measured by the Cls main to shake-up area ratio.

5.3 POLY(STYRENE-DIENE-STYRENE) SYSTEM: VALENCE BAND ANALYSIS

As was noted in the previous section the analysis of the shake-up peaks left the question of surface orientation of the diene blocks unanswered. Shake-up peaks arise from valence level transitions induced by core level photoionization. However, valence band peaks arise from direct valence band photoionization, and can give more direct information on the valence band structure. Therefore, a study of the valence band peaks was undertaken to verify and clarify the trends observed by shake-up analysis.

The valence band spectra for the SBS and SIS system are shown in Figure 25 and Figure 26. The valence band spectra for SBS, as well as its components, PS and PB, are displayed in Figure 25. The valence band spectra for SIS, as well as its components, PS and PI, are displayed in Figure 26. Although no published valence band spectra are available for PI, both PS and PB valence band spectra have been collected and published by J. J. Pireaux, et al.⁵³. The spectra presented by Pireaux, et al. and the spectra presented in

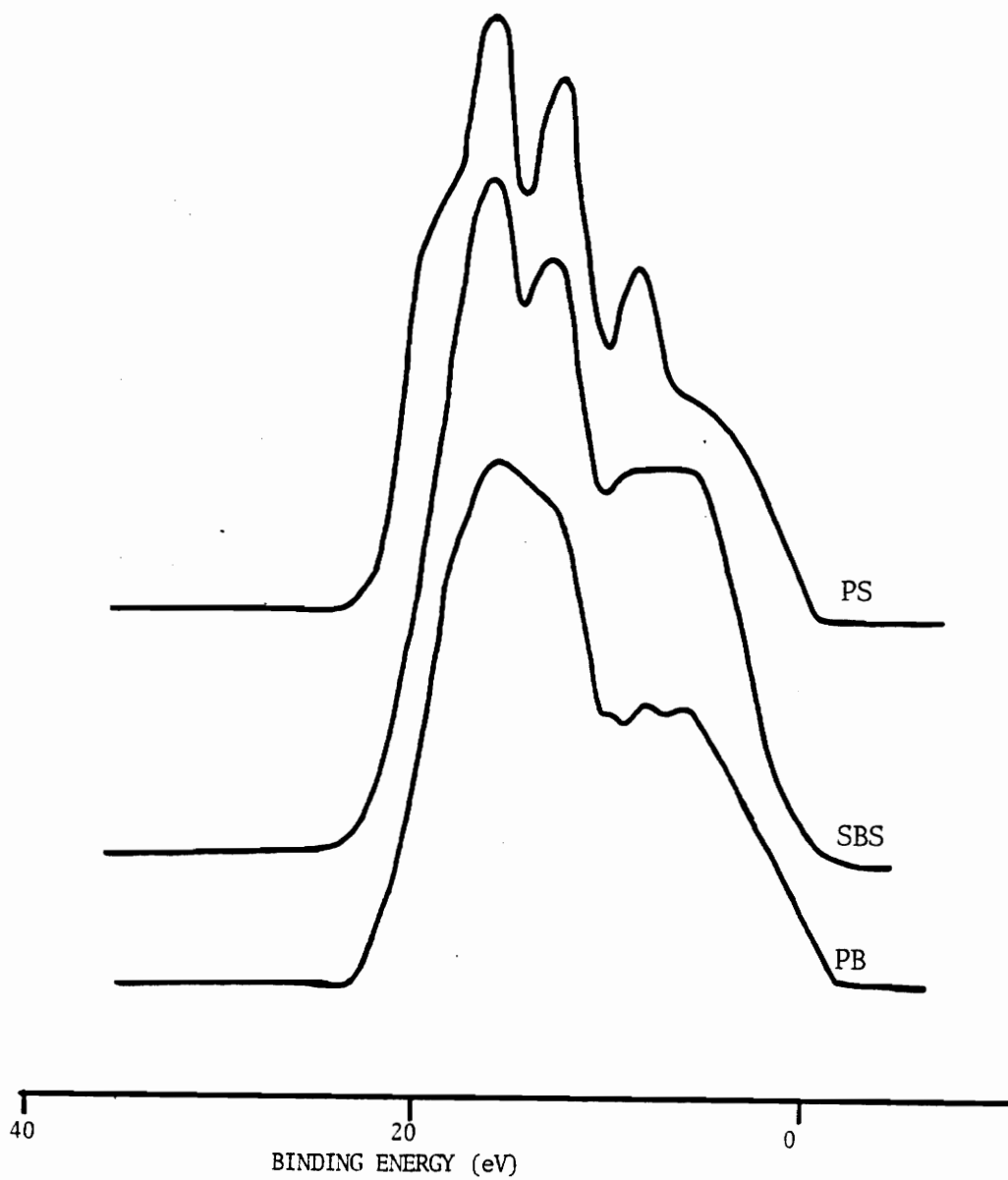


Figure 25. Valence Band Spectra - SBS

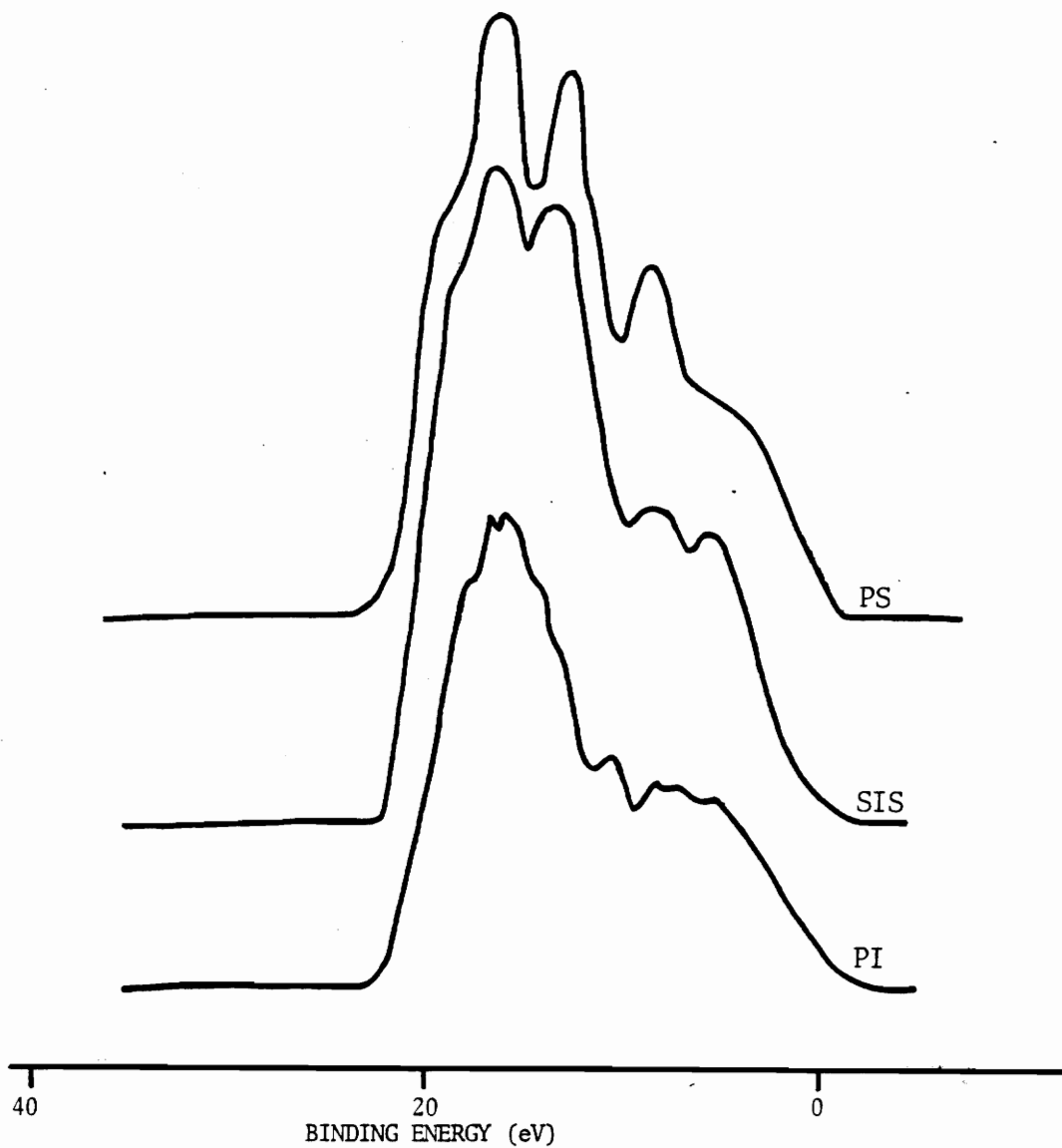


Figure 26. Valence Band Spectra - SIS

Figure 25 agree well if experimental and data processing factors are taken into account. Pireaux, et al. used monochromatic aluminum X-rays, while polychromatic magnesium X-rays were used in the current study. Therefore, the spectra presented in this work are expected to be much less resolved than the literature spectra. Pireaux, et al. also presented their spectra before the baseline was subtracted, while the spectra are presented after a non-linear baseline was subtracted in the present study. If those two factors are taken into account, the spectra in this study and those of Pireaux, et al. agree well. Both sets of spectra have the same number of peaks, same relative peak positions, (very similar absolute peak positions, as well), and similar relative heights of the peaks (using a linear baseline on the literature spectra).

The key to understanding the valence band is the assignment of the peaks through MO (molecular orbital) models of similar compounds. Pireaux, et al.⁵⁴ used this technique to establish the MO corresponding to the main peaks in the spectrum of polystyrene based on benzene as the model compound. This assignment is shown in Figure 27, the pictorial MOs of benzene corresponding to these peaks are shown in Figure 28. In the present study a similar tactic was used, the valence bands of butadiene and isoprene were compared to the closest model compound match that was found, which was trans-2-butene. The spectra for PB and PI are shown in Fig-

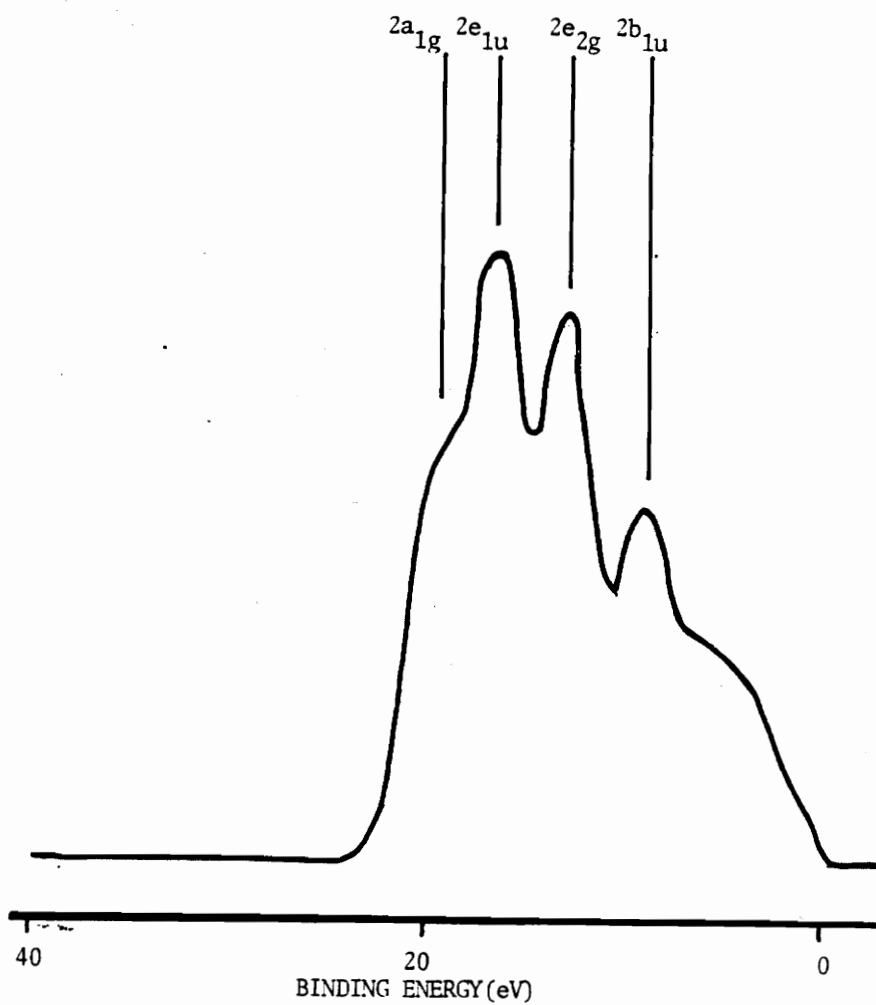


Figure 27. MO Assignments for Polystyrene

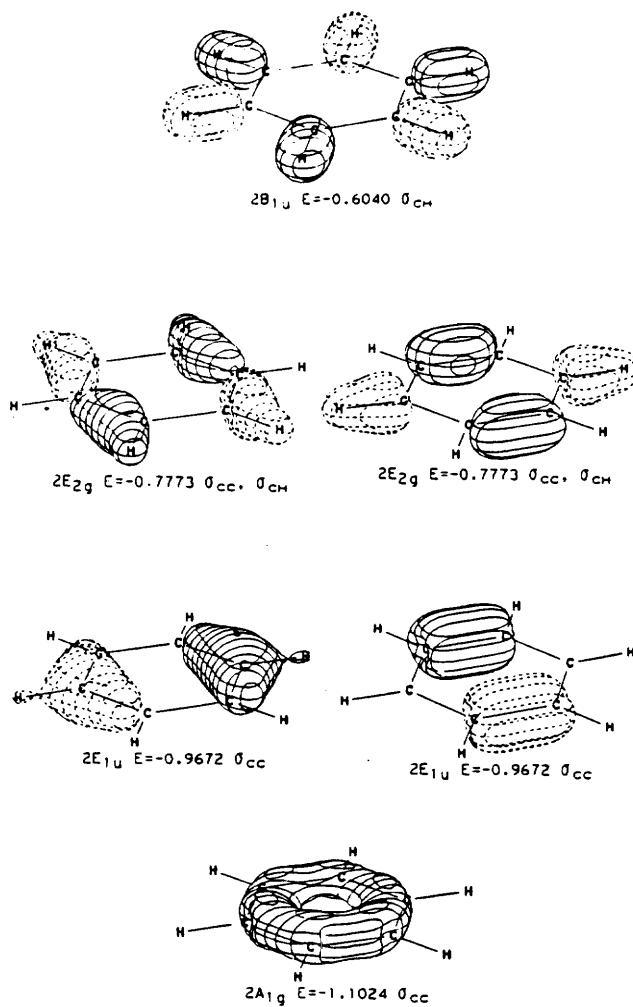


Figure 28. Pictorial MOs for Benzene: (From Jorgensen and Salem⁵ pages 257 and 258).

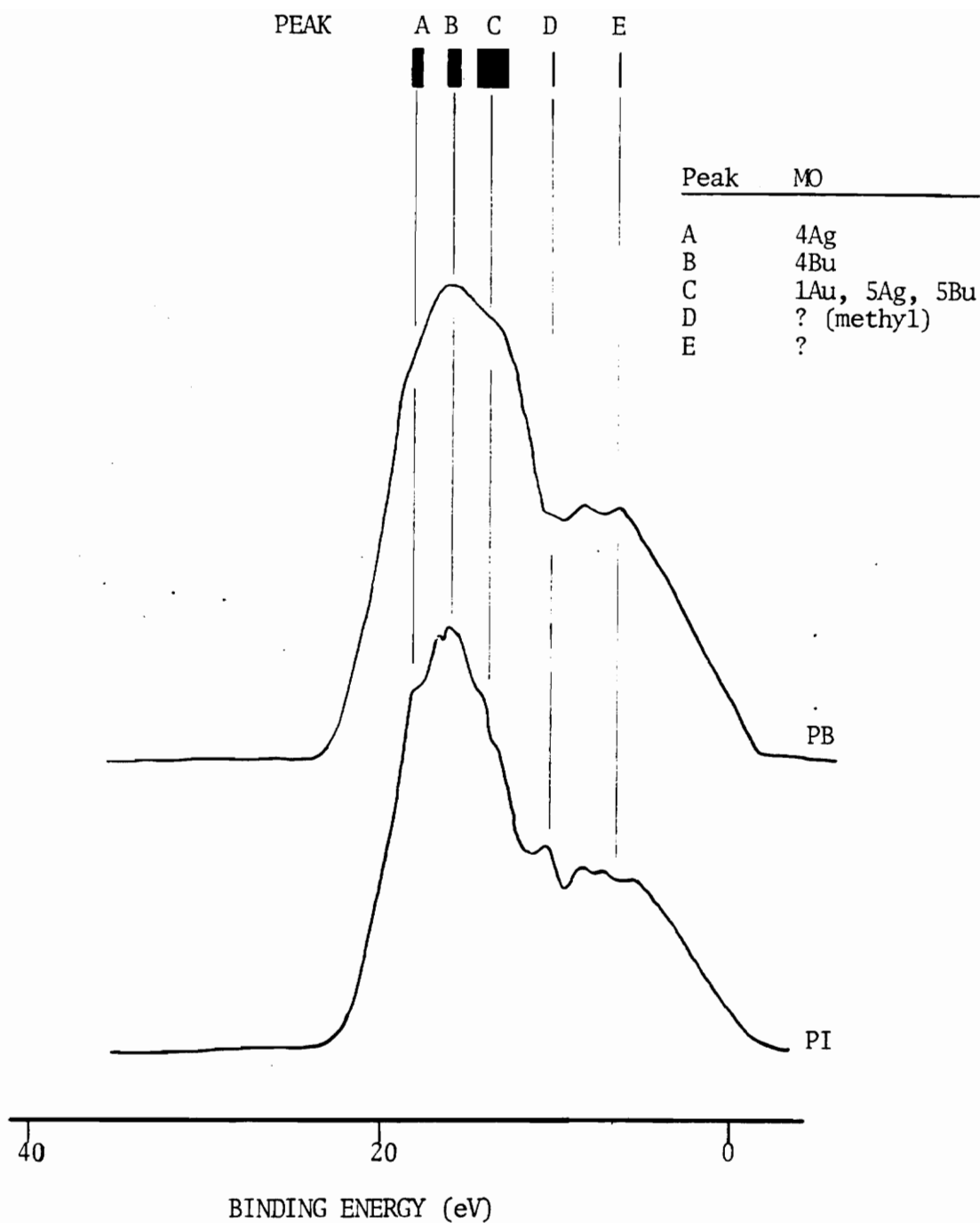


Figure 29. MO Assignments for Polybutadiene and Polyisoprene

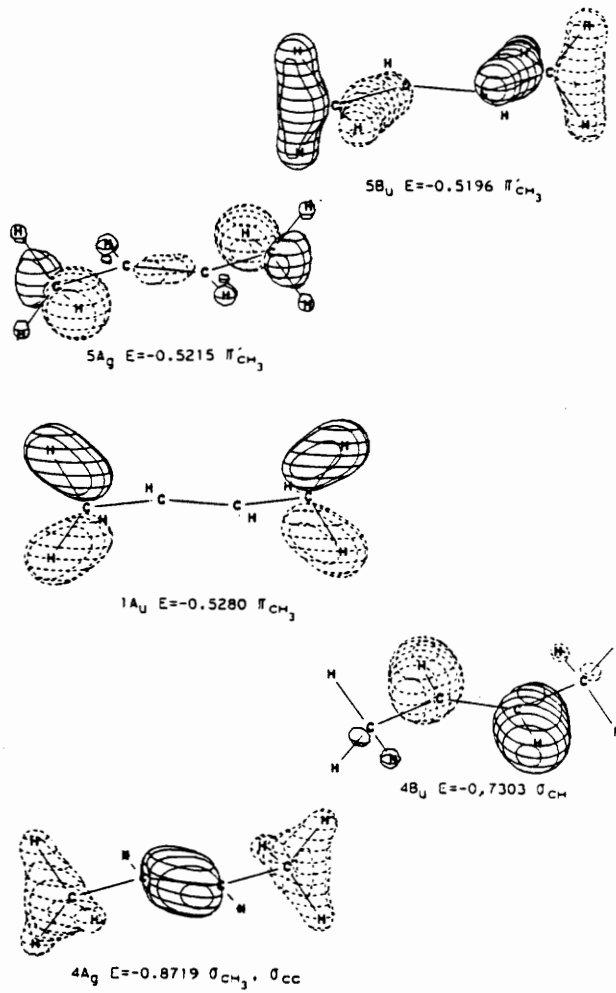


Figure 30. Pictorial MOs for Trans-2-Butene: (From Jorgensen and Salem^{5,8} pages 210 and 211).

ure 29 with the assignments based upon the MOs of trans-2-butene which are shown in Figure 30. The extra peak (D) in the PI spectra may be due to the methyl side group on the PI repeat unit that is absent on the PB repeat unit. However, using the analog between PI and PB, and polypropylene and polyethylene, (see chapter 3, Figure 6) there is very likely an unresolved peak under the main set of peaks, in the range of 15 to 18 eV which also corresponds to the methyl side group.

A point of concern was the sensitivity of the valence band to fine detail such as cis or trans stereoisomerism. Pireaux, et al.⁵³ stated that experiments they had performed to distinguish the valence band of cis versus trans stereoisomers of poly(1,4-dichloro-2,3-epoxybutene) and polyisoprene were unsuccessful. The cis and trans isomers were undistinguishable. However, they did indicate that preliminary results just acquired for cis versus trans poly(1,4-butadiene) showed substantial modifications in the valence band. However, the publication promised in 1981 detailing this variation has not yet appeared. Consequently, although the matter is not at all clear, indications are that cis versus trans stereoisomers are indistinguishable in the valence band as measured by XPS. This was a point of concern since the stereoisomeric forms of the diene polymers and diene blocks were not known.

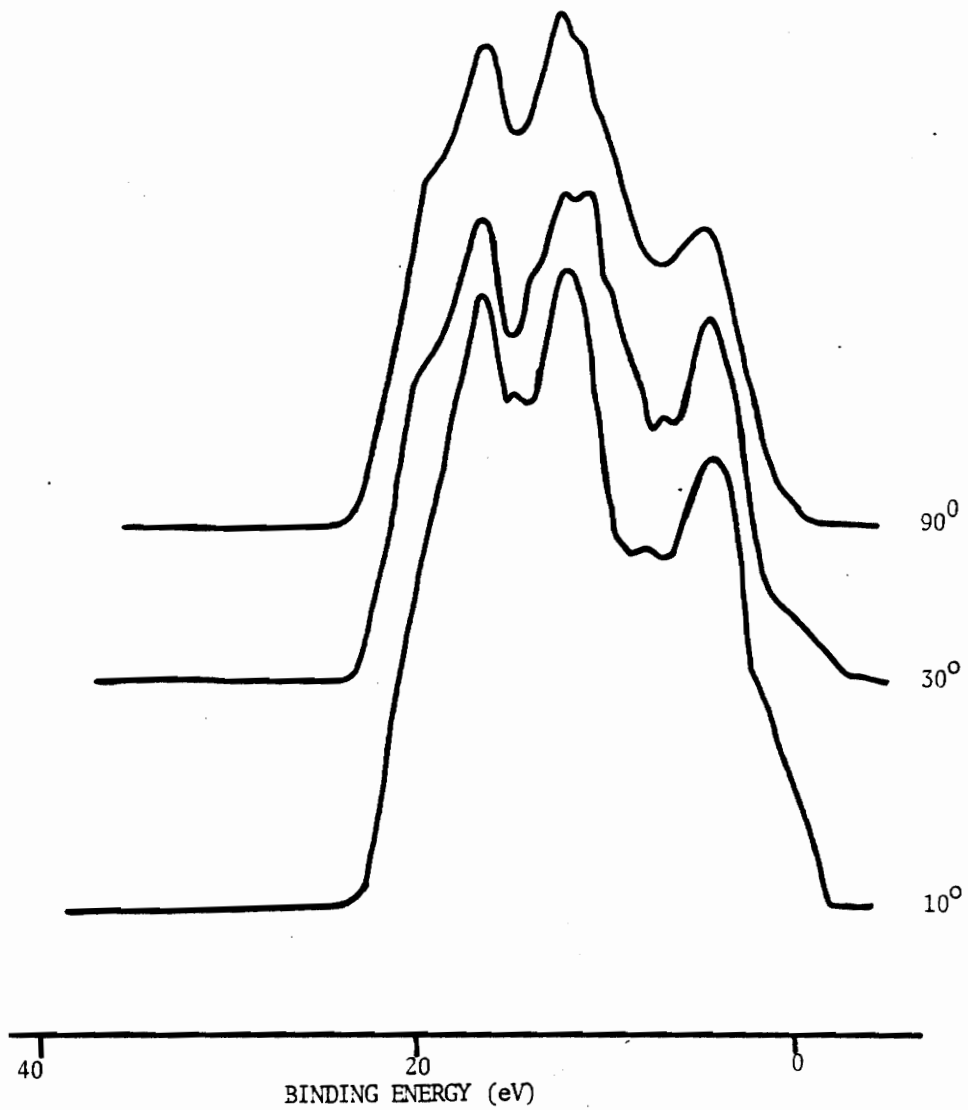


Figure 31. Valence Band Spectra for Toluene Fast Cast
- SBS

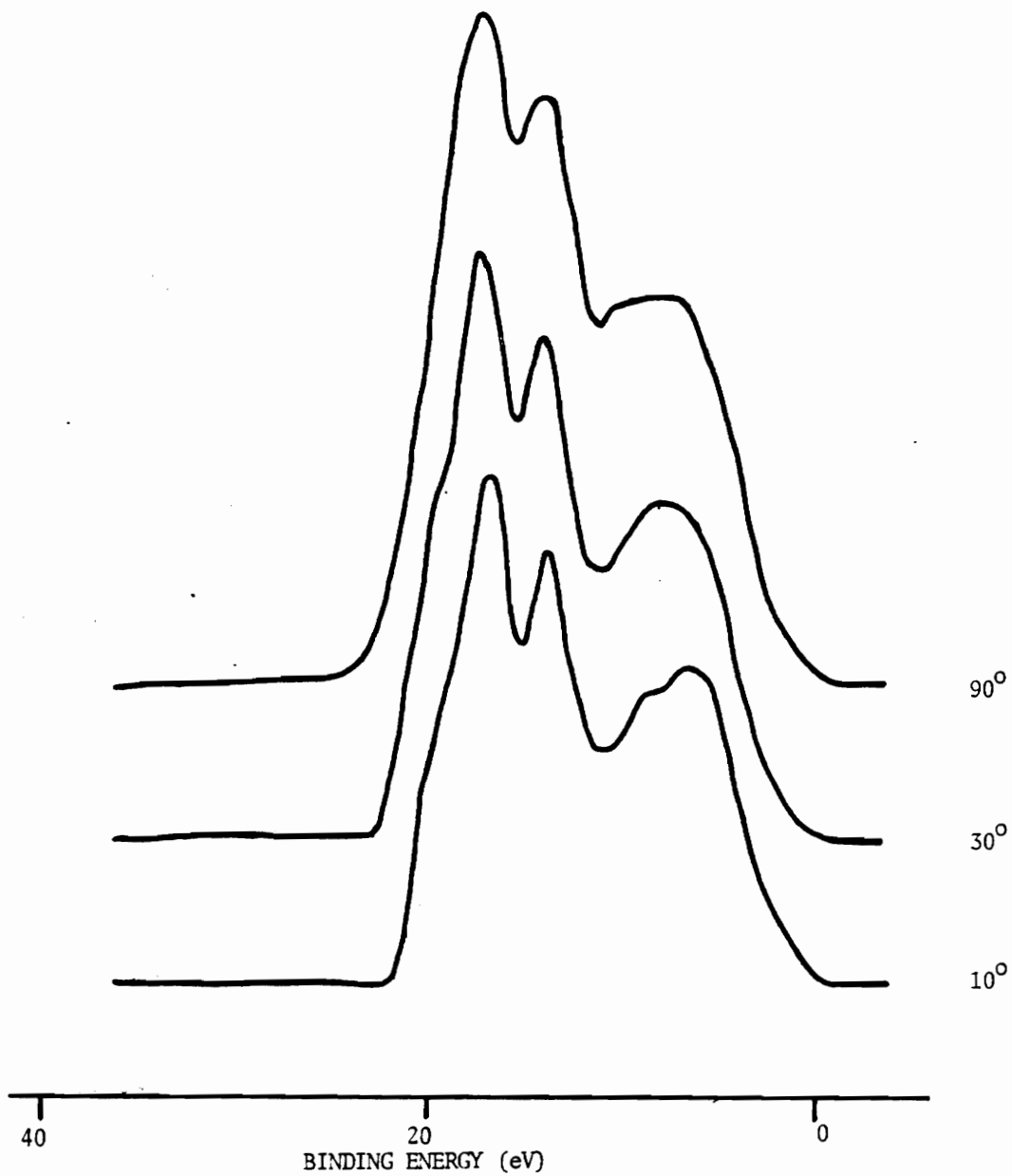


Figure 32. Valence Band Spectra for Toluene Slow Cast - SBS

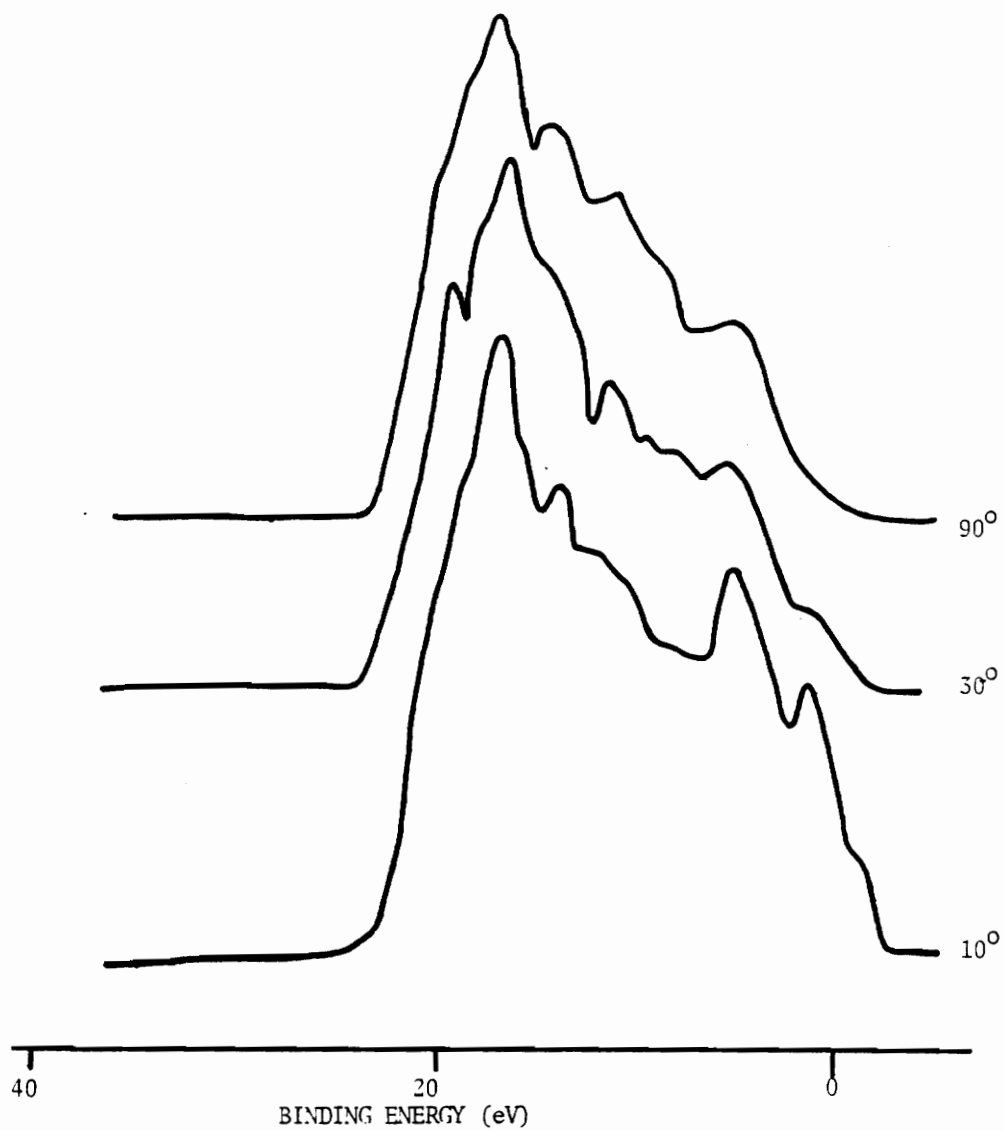


Figure 33. Valence Band Spectra for Toluene Fast Cast - SIS

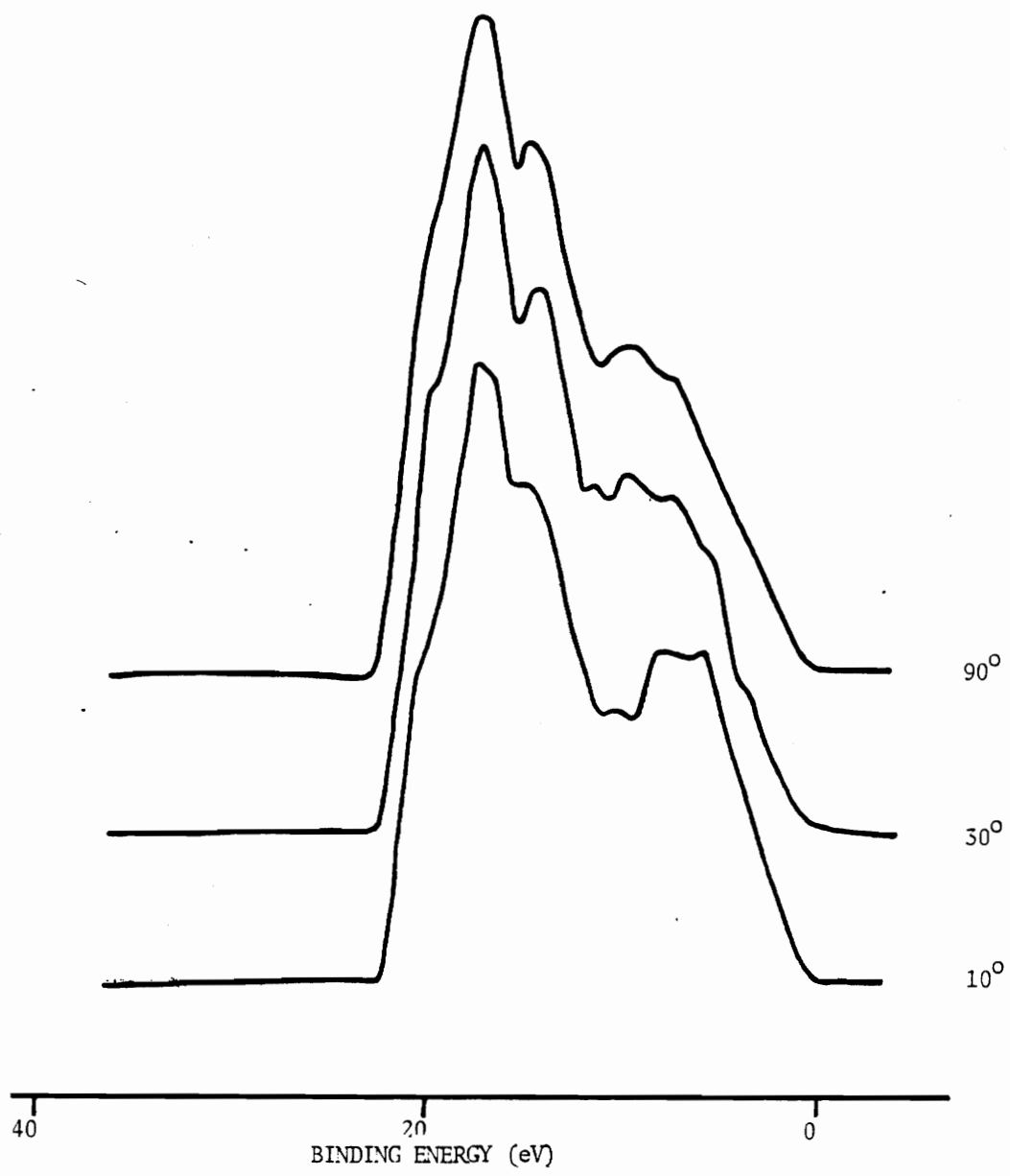


Figure 34. Valence Band Spectra for Toluene Slow Cast - SIS

Valence band spectra were collected at three angles of analysis on block copolymers cast from toluene at a slow rate and at a fast rate of solvent evaporation. Shown in Figure 31 and Figure 32 are the spectra for SBS cast at a fast rate and at a slow rate, respectively. Shown in Figure 33 and Figure 34 are the corresponding spectra sets for SIS.

In order to analyze the valence band spectra the relative heights at the assigned MO energies were measured. The analysis was performed to determine whether orientation of the polymer existed at the surface. This in turn would affect the concentration profiles obtained by shake-up analysis. The peak height measurements were made relative to peak B (height of peak B = 100). The results for the SBS copolymer are shown in Figure 35 and for the SIS copolymer in Figure 36. As can be seen by comparing the curves on Figure 35, peaks A and C decline slightly relative to peak B as the surface is approached. This indicates that the MOs corresponding to peak B are slightly more favorably oriented toward the surface. This would correspond to an orientation model as shown in Figure 37. A similar comparison of the curves for the SIS copolymer shows a less clear-cut situation. However, peak A clearly declines relative to peak B as the surface is approached. This indicates that the pi-bonds associated with peak A are deeper into the surface than the alkane-like segments corresponding to peak B. The fact

that peak D is less intense for the slow toluene cast film than for the fast toluene cast film may indicate that the methyl groups are not surface segregating. Using both of these observed factors, a surface model similar to that for the butadiene blocks can be made, as shown in Figure 38.

Both of these orientations are reasonable due to the lower surface energy of this configuration. These orientation models are supported by angular dependent valence band spectra collected on neat polybutadiene and neat polyisoprene. This orientation observed for the homopolymers explains the aforementioned depth variations of the shake-up to main ratios.

As a consequence of this determination of the orientation, the steep gradient found on the shake-up analysis results at the near surface can more easily be understood. The high pi-bond concentration from 90° and 30° spectra is in part due to the high concentration of pi-bonds from the diene. Since the diene is oriented at the surface the 10° (and to some extent 30°) scans will detect low concentrations of pi-bonds and high concentrations of alkane-type carbon bonds. At 90° the depth of analysis is greatly increased and the pi-bonds of the surface oriented diene units are detected. These pi-bonds cause an increase in the shake-up intensity relative to the Cls peak, and thus the pi-bond concentration increases. Therefore, the curves presented in

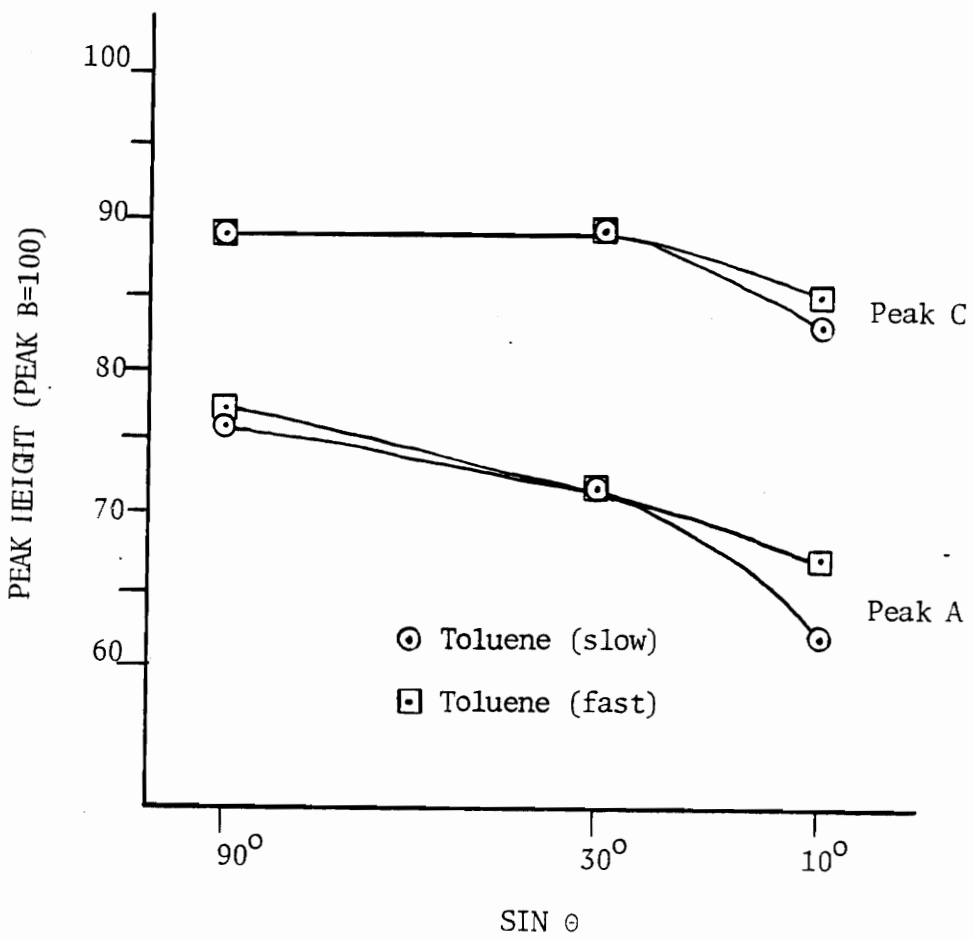


Figure 35. Relative Peak Heights for the SBS Copolymer

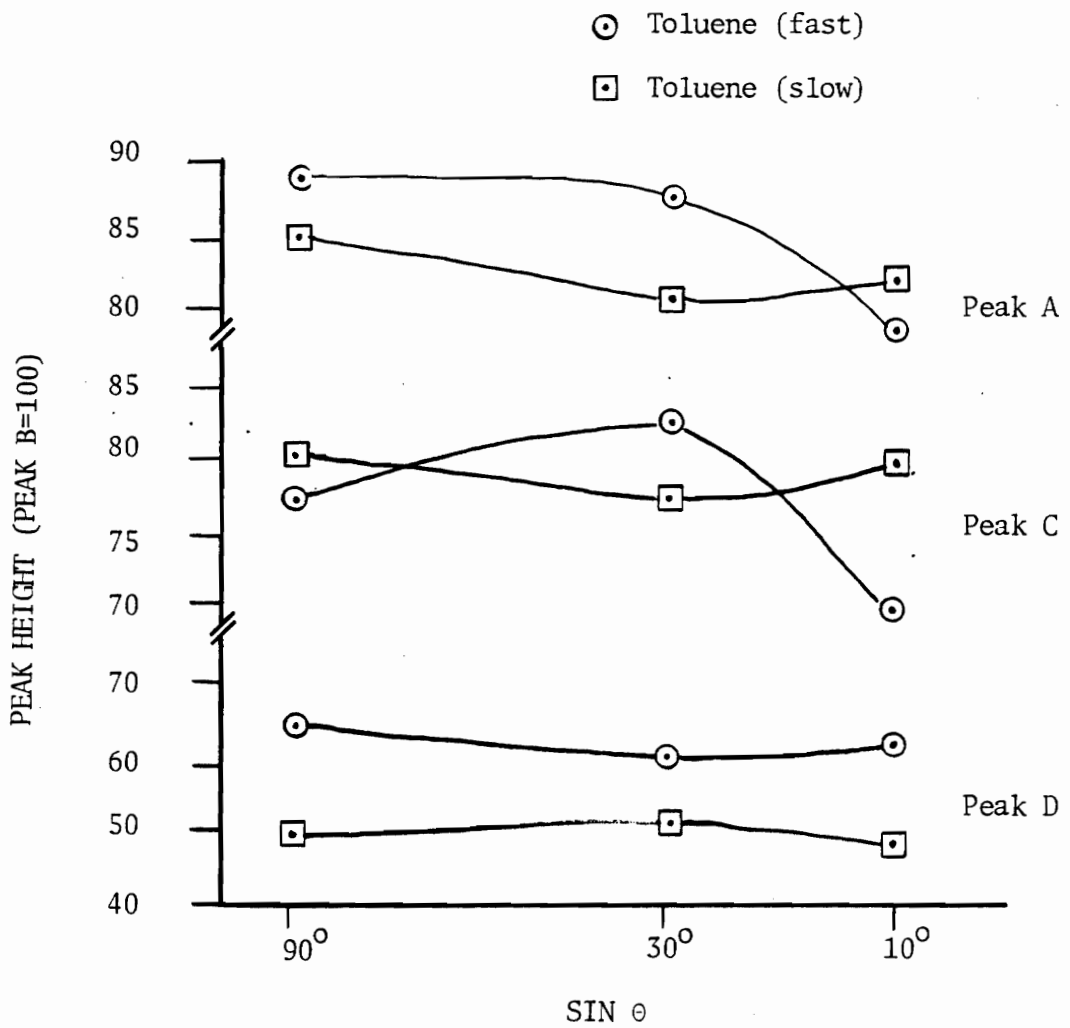


Figure 36. Relative Peak Heights for the SIS Copolymer

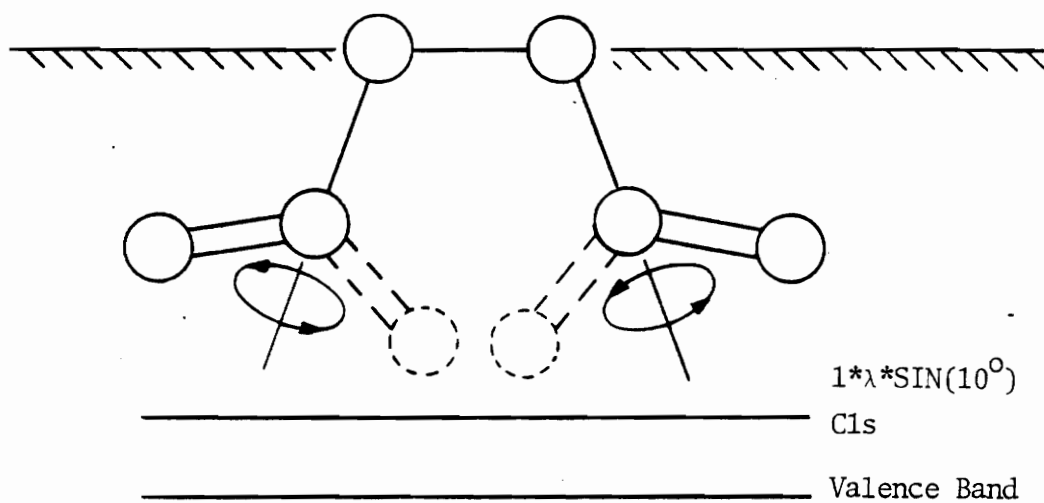


Figure 37. Orientation Model For Butadiene Repeat Units at the Surface

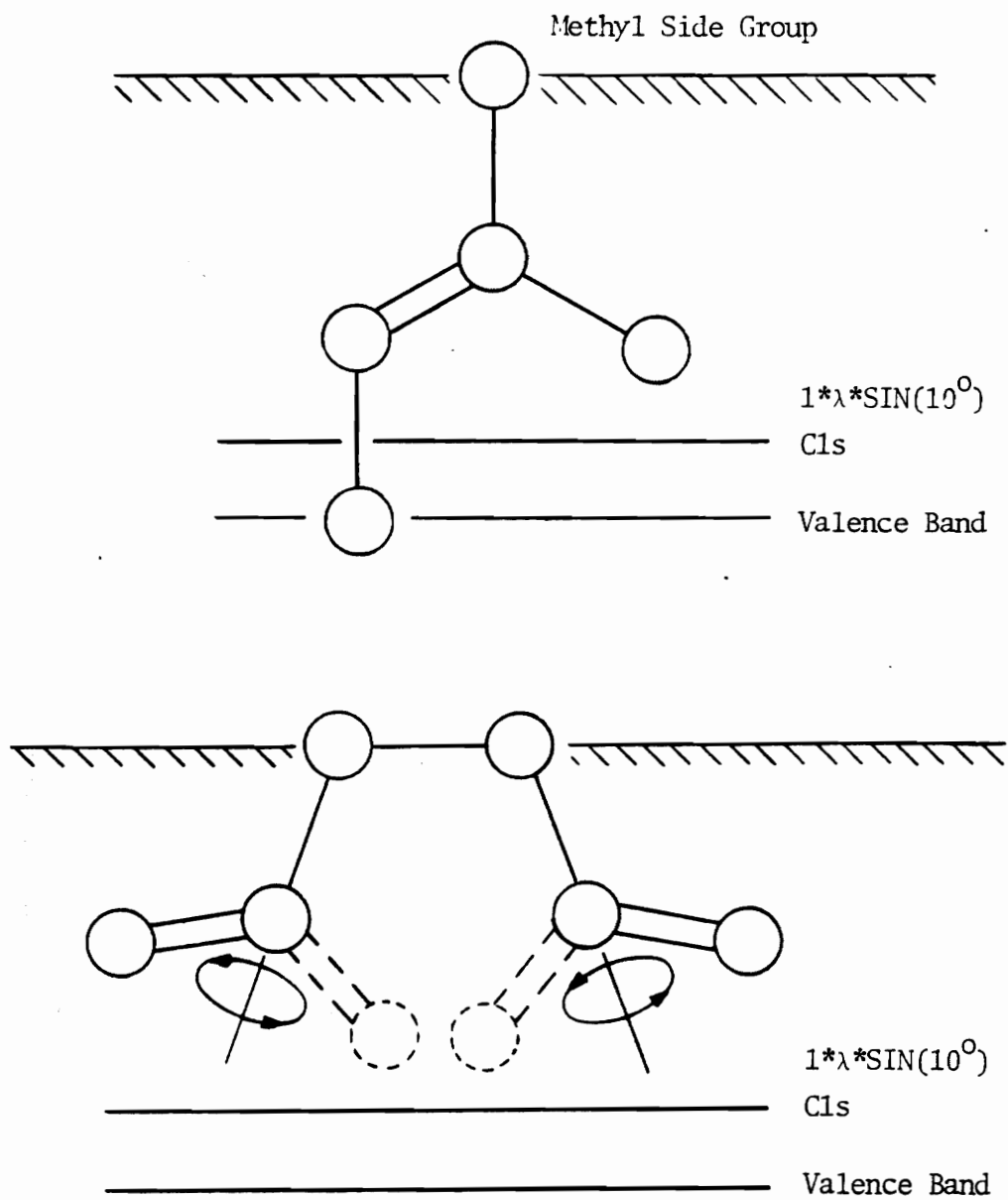


Figure 38. Orientation Models For Isoprene Repeat Units at the Surface

the previous chapter can be used only on a semi-quantitative basis.

The general comments that can be made as a result of the valence band analysis are comments about the orientation of the diene blocks at the surface. Both isoprene, and butadiene repeat units are preferentially oriented at the surface with the pi-bonds away from the surface. The surface thus appears full of =CH₂ and -CH₃ groups. As a result of this orientation the shake-up analysis is slightly altered, and hence it is only a semi-quantitative measure of surface segregation.

6.0 SUMMARY

The results of the present work can be summarized as follows for the siloxane-sulfone system:

- In every film prepared very strong siloxane surface segregation was observed.

- As the rate of solvent evaporation was increased the siloxane concentration deeper into the surface decreased, however the surface concentration remained the same. This is probably the result of the decreased time for polymer rearrangement and phase separation at the surface. The surface concentration remains constant because of the large driving force for siloxane surface segregation.

- Data presented by other experimenters shows that the casting solvent does affect the surface concentration profile. Solvents with high vapor pressures and which are selective to siloxane blocks produce a thinner siloxane overlayer. Solvents with low vapor pressures and which are selective to PS produce thicker siloxane overlayers.

- The interfaces formed against two substrates gave very different results. The interface formed against mercury had a siloxane concentration nearly the same as the air surface, however the concentration gradient was much steeper on the mercury side. This is probably the result of the mercury-

polymer interfacial energy being minimized by siloxane segregation, and electronic interactions between the mercury and the sulfone block. The interplay between those two driving forces causes the siloxane gradient to steepen while the surface concentration remains the same as the air side. The interface formed against water had a lower siloxane concentration than the air side, however the concentration profiles had similar slopes. This may be due to sample preparation factors such as bulk composition, the ultrafast rate of film formation, or solution-water interactions. Or perhaps minimizing the interfacial energy on the water side may occur with less than complete siloxane segregation.

The results of the present work on the SDS system can be summarized as follows:

- In every film prepared surface segregation of the butadiene or isoprene blocks was detected.

- Analysis of the valence band showed that methylene groups or methyl side groups orient at the surface and the pi-bonds are oriented deeper into the polymer.

- The degree of surface segregation increases as the evaporation rate decreases. Both the surface concentration and the concentration gradient vary with the evaporation rate.

- The degree of surface segregation increases as the solvent-PS compatibility decreases. Films cast from THF have a larger than expected surface concentration of the diene block as compared to the toluene films. The effects of the solvent-diene incompatibility counteract the faster evaporation rate of the THF.

There were some limitations to the present work. Most of the films studied were non-equilibrium films, consequently there is some experimental uncertainty concerning the exact state of the film. Also, this study did not investigate the variations in surface texture which may occur with the variations in processing factors. Consequently, it is not known if the surface profiles measured are actual chemistry profiles, the effects of surface microdomain morphology and texture, or a combination of both.

7.0 CONCLUSIONS

As result of the present work several conclusions about the effects of casting parameters on the surface of block copolymer containing films can be made. In general, the closer the approach to equilibrium, the more completely covered the surface is in the lower surface energy block. However, non-equilibrium conditions brought about by fast evaporation, or solvent-polymer incompatibility alter the surface concentration profile of the polymer.

In the siloxane-sulfone system the easily quantified results indicate a high degree of siloxane surface segregation which varies with evaporation rate, and substrate. The effect of a fast evaporation rate is that the surface becomes immobilized more rapidly and diffusion of siloxane blocks is inhibited (by the immobilized sulfone blocks). The effects of casting substrate are evidently quite complicated and dependent upon the specific substrate. Important factors are the substrate-block interactions, substrate-solution interactions, and the substrate-polymer interfacial energy.

In the styrene-diene-styrene system the lower surface energy component, isoprene or butadiene, segregates to the surface of the copolymer film. The degree of this segregation as measured by the shake-up to main peak area ratio increases for slow evaporation rates. The degree of this

segregation is also greatly increased when the diene-solvent incompatibility increases. The diene is then driven to the surface by the lowering of surface energy driving force, as well as the heat of mixing driving force repelling the the diene from the solvent-rich center of the film. A study of the valence band revealed that the diene repeat units orient at the surface such as to present =CH₂ and -CH₃ groups to the surface, while orienting the pi-bonds towards the bulk.

8.0 REFERENCES

- ¹ H. W. Bonk, "Thermoplastic Elastomers" in Modern Plastics Encyclopedia, 61-no.10A, 100, (1984).
- ² J. H. Sanders, *Rubber Rev.*, 33, 1293, (1960).
- ³ D.M. Brewis, in Surface Analysis and Pretreatment of Plastics and Metals, Edited by D. M. Brewis. Page 1. (1982).
- ⁴ P. O. Sherman, S. Smith, and B. Jahannessian, *Textile Res. J.*, 39, 449, (1969).
- ⁵ D. F. Kagen, V. V. Prokopenko, Y. M. Malinskii, and N. F. Bakeyev, *Polymer Science - USSR*, 32, 124, (1972).
- ⁶ J. Schultz, K. C. Sehgal, and M. E. R. Shanahan, in Adhesion 1. Edited by K. W. Allen. Page 269. (1977).
- ⁷ M. J. Owens, and J. Thompson, *British Polymer Journal*, 4, 297, (1972).
- ⁸ D. McIntyre, and E. Campos-Lopez, in Block Polymers. (Plenum Press: New York, 1970). Pages 19-30.
- ⁹ M. Matsuo, and S. Sagaye, in Colloidal and Morphological Behavior of Block and Graft Copolymers. Edited by G. E. Molau. (Plenum Press: New York, 1971). Pages 1-19.
- ¹⁰ E. B. Bradford, in Colloidal and Morphological Behavior of Block and Graft Copolymers. Edited by G. E. Molau. (Plenum Press: New York, 1971). Pages 21-31.
- ¹¹ J. C. Saam, and F. W. G. Fearon, *Ind. Eng. Chem. Prod. Res. Develop.*, 10-no.1, 10, (1971).
- ¹² P. Bajaj, D. C. Gupta, and S. K. Varshney, *Polymer Engineering and Science*, 23-no.15, 820, (1983).
- ¹³ S. Bagrodia, and G. L. Wilkes, *J. Biomed. Mater. Res.*, 10, 101, (1976).
- ¹⁴ F. S. Bates, C. V. Berney, and R. E. Cohen, *Macromolecules*, 16, 1101, (1983).
- ¹⁵ H. Hashimoto, M. Fujimura, T. Hashimoto, and H. Kawai, *Macromolecules*, 15, 844, (1981).

- ¹⁶ E. R. Pico, and M. C. Williams, *J. Polym. Sci., Polym. Phys. Ed.*, 15, 1585, (1977).
- ¹⁷ G. E. Molau, and W. M. Wittbrodt, *Macromolecules*, 1-no.3, 260, (1968).
- ¹⁸ G. E. Molau, in Colloidal and Morphological Behavior of Block and Graft Copolymers. Edited by G. E. Molau. (Plenum Press: New York, 1971). Pages 79-105.
- ¹⁹ T. Inoue, T. Soen, T. Hashimoto, and H. Kawai, *J. of Polymer Science: Part A-2*, 7, 1283, (1969).
- ²⁰ J. V. Dawkins, in Block Copolymers. (Applied Science: London, 1973). Pages 409-442.
- ²¹ J. V. Dawkins, in Block Copolymers. (Applied Science: London, 1973). Pages 363-408.
- ²² A. Noshay, and J. E. McGrath, in Block Copolymers: Overview and Critical Survey. (Academic Press: New York, 1977).
- ²³ R. E. Cohen, and F. S. Bates, *J. of Polymer Science: Polymer Physics Ed.*, 18, 2143, (1980).
- ²⁴ D. G. LeGrand, and G. L. Gaines, *Polymer Preprints*, 11, 442, (1970).
- ²⁵ G. L. Gaines, and G. W. Bender, *Macromolecules*, 5, 1101, (1972).
- ²⁶ G. L. Gaines, *Macromolecules*, 12, 1101, (1979).
- ²⁷ D. H. Kaelble, E. H. Arlin, and M. Shen, in Colloidal and Morphology Behavior of Block and Graft Copolymers. Edited by G. E. Molau. (Plenum Press: New York, 1971). Page 295-306.
- ²⁸ Y. Yamashita, *J. Macromol. Sci.-Chem.*, A13-no.3, 401, (1979).
- ²⁹ E. B. Bradford and E. Vanzo, *J. of Polymer Science: Part A-1*, 6, 1661, (1968).
- ³⁰ R. G. Crystal, P. F. Erhardt, and J. J. O'Malley, in Block Copolymers. Edited by S. L. Aggarwal. (Plenum Press: New York, 1970). Pages 179-193.
- ³¹ J. S. Riffle, Ph. D. Thesis, VPI&SU, (1980).

- ³² J. E. McGrath, D. W. Dwight, J. S. Riffle, T. F. Davidson, D. C. Webster, and R. Viswanathan, *Polymer Preprints*, 20-no.2, 528, (1979).
- ³³ D. W. Dwight, B. Beck, J. S. Riffle, and J. E. McGrath, *Polymer Preprints*, 20-no.1, 702, (1979).
- ³⁴ A. K. Sha'aban, M. S. Thesis, VPI&SU, (1983).
- ³⁵ H. R. Thomas, and J. J. O'Malley, *Macromolecules*, 14-no.5, 1316, (1981).
- ³⁶ H. R. Thomas, and J. J. O'Malley, *Macromolecules*, 12-no.2, 323, (1979).
- ³⁷ J. J. O'Malley, H. R. Thomas, H. Ronald, and G. M. Lee, *Macromolecules*, 12-no.5, 996, (1979).
- ³⁸ D. Briggs, in Electron Spectroscopy: Theory, Techniques, and Applications. Edited by C. R. Brundle and A. D. Baker. (Academic Press: New York, 1979). Volume 3, page 306.
- ³⁹ C. D. Wagner, W. M. Riggs, L. E. Davis, J. F. Moulder, and G. E. Muilenberg. Handbook of X-Ray Photoelectron Spectroscopy. (Perkin-Elmer Corp.: Eden Prairie, MN, 1979). Pages 4-6.
- ⁴⁰ C. J. Powell, *Surface Science*, 44, 29, (1974).
- ⁴¹ J. E. Castle, and R. H. West, *J. Elect. Spectro. Rel. Phenom.*, 19, 409, (1980).
- ⁴² D. T. Clark, and H. R. Thomas, *J. Polymer Sci.: Polymer Chem. Ed.*, 15, 2843, (1977).
- ⁴³ J. Szajman, and R. C. G. Leckey, *J. Elect. Spectro. Rel. Phenom.*, 23, 83, (1981).
- ⁴⁴ J. Szajman, J. Liesegang, J. G. Jenkin, and R. C. G. Leckey, *J. Elect. Spectro. Rel. Phenom.*, 23, 97, (1981).
- ⁴⁵ D. R. Penn, *J. Elect. Spectro. Rel. Phenom.*, 9, 29, (1976).
- ⁴⁶ D. Briggs, in Handbook of X-Ray and Ultraviolet Photoelectron Spectroscopy. Edited by D. Briggs. (Heyden: Philadelphia, 1978). Pages 153-181.

- ⁴⁷ J. H. Scofield, *J. Elect. Spectro. Rel. Phenom.*, 8, 129, (1976).
- ⁴⁸ R. S. Reilman, A. Msezane, and S. T. Manson, *J. Elect. Spectro. Rel. Phenom.*, 8, 389, (1976).
- ⁴⁹ D. T. Clark, A. Dilks, J. Peeling, and H. R. Thomas, *Faraday Discussions of the Chemical Society*, 60, 183, (1975).
- ⁵⁰ D. T. Clark, and A. Dilks, *J. Polymer Sci.: Polymer Chem. Ed.*, 14, 533, (1976).
- ⁵¹ D. T. Clark, D. B. Adams, A. Dilks, J. Peeling, and H. R. Thomas, *J. Elect. Spectro. Rel. Phenom.*, 8, 51, (1976).
- ⁵² D. T. Clark, and A. Dilks, *J. Polymer Sci.: Polymer Chem. Ed.*, 15, 15, (1977).
- ⁵³ J. J. Pireaux, J. Riga, R. Caudano, and J. J. Verbist, in Photon, Electron, and Ion Probe of Polymer Structure and Properties. Edited by D. W. Dwight, T. J. Fabish, and H. R. Thomas. (ACS: Washington, 1981). Pages 169-201.
- ⁵⁴ J. J. Pireaux, J. Riga, R. Caudano, J. J. Verbist, J. Delhalle, S. Delhalle, J. Andre, and Y. Gobillon, *Physica Scripta*, 16, 329, (1977).
- ⁵⁵ W. R. Salaneck, *CRC Critical Rev. in Solid State Sci.*, in press, (1985). (Plenum Press: New York, 1970). Pages 19-30.
- ⁵⁶ N. M. Patel, M. S. Thesis, VPI&SU, (1984).
- ⁵⁷ E. A. Corragin, working under D. W. Dwight in the Winter and Spring of 1985.
- ⁵⁸ W. L. Jorgensen and L. Salem. The Organic Chemist's Book of Orbitals. (Academic Press: New York, 1973).

APPENDIX A. NON-LINEAR BASELINE SUBTRACTION PROGRAM

Below is the listing of the computer program written to perform the non-linear baseline subtraction as described in Chapter 3.

```
C
C   PROGRAM TO CHARGE CORRECT AND SUBTRACT THE
C   NON-LINEAR BASELINE FROM VALENCE BAND XPS
C   SPECTRA.  THE INPUT IS 400 INTENSITY VALUES
C   TAKEN EVERY 0.1EV FROM 40.0 TO 0.0EV.
C
  DIMENSION XRAW(400), DELCPS(400), XFINAL(400)
  DIMENSION XRAWI(400), DCPS2(400)
  CHARACTER*72 ID
  READ(1,100)ID
  READ(1,*)CHARGE
  ICHARG=CHARGE*10
  WRITE(2,100)ID
  READ(1,*) (XRAW(J), J=1,400,1)
  DO 115 J=1,400,1
115   XRAWI(J)=XRAW(J)
  DO 120 J=1,400,1
120   IF(XRAW(J).LT.0.0) GOTO 121
121  XRAW(J)=ABS(XRAW(J))
     JSTAR=J
C
C   CALCULATE THE AREA FROM JSTAR ON TO J=400
C   AND SUBTRACT LINEAR BASELINE.  (JSTAR IS
C   THE BACKGROUND NOISE POINT ON THE HIGH B.E.
C   SIDE OF THE SPECTRUM - CHOSEN BY THE USER.)
C
  AREA=0.5*(XRAW(JSTAR)+XRAW(400))
  DELTAY=XRAW(JSTAR)
  DO 130 J=JSTAR+1,399,1
130   AREA=AREA+.1*XRAW(J)
     AREA=AREA-0.05*DELTAY*(400-JSTAR)
  DO 132 J=1, JSTAR, 1
132   DELCPS(J)=DELTAY
  DO 134 J=JSTAR, 400, 1
134   DELCPS(J)=DELTAY*(1-FLOAT(J-JSTAR)/FLOAT(400-JSTAR))
  DO 136 J=1, 400, 1
     XRAW(J)=XRAW(J)-DELCPS(J)
136   IF(XRAW(J).LT.0.0)XRAW(J)=0.0
     DELCPS(400)=0.0
C
C   NON-LINEAR SUBTRACTION LOOP
C
138  DCPS2(400)=0.0
     TALLY=0.0
     DO 140 J=399, JSTAR, -1
```

```

    TALLY=TALLY+.05*(XRAW(J+1)+XRAW(J))
140  DCPS2(J)=DELTAY*TALLY/AREA
    DELSUM=0.0
    IDEL=0.0
    DO 150 J=JSTAR,400,1
        IF(DCPS2(J).LT.1.)GOTO 150
        IDEL=IDEL+1
        DELSUM=DELSUM+ABS((DCPS2(J)-DELCPS(J))/DCPS2(J))
150  DELCPS(J)=DCPS2(J)
    DO 160 J=1,400,1
        XRAW(J)=XRAWI(J)-DELCPS(J)
160  IF(XRAW(J).LT.0.0)XRAW(J)=0.0
    IF(DELSUM/IDEL.GT..005)GOTO138
C
C  CHARGE CORRECTION
C
    IF(ICHARG.EQ.0)GOTO 220
    IF(ICHARG.LT.0)THEN
        ICHARG=ABS(ICHARG)
        DO 170 J=1,ICHARG,1
170     XFINAL(J)=0.0
        DO 180 J=ICHARG,400,1
180     XFINAL(J)=XRAW(J-ICHARG+1)
    ELSE
        DO 190 J=1,400-ICHARG,1
190     XFINAL(J)=XRAW(J+ICHARG)
        DO 200 J=400-ICHARG,400,1
200     XFINAL(J)=0.0
    END IF
210 WRITE(2,110)(XFINAL(J),J=1,400,1)
    STOP
220 WRITE(2,110)(XRAW(J),J=1,400,1)
    STOP
100 FORMAT(A72)
110 FORMAT(10(F6.0,1X))
    END

```

APPENDIX B. SILOXANE QUANTIFICATION: EQUATION DEVELOPMENTS

The following are the developments of the equations used to convert the area ratios into weight percent siloxane.

Since there is one silicon atom per repeat unit and the repeat unit weight is 74 g/mol, then:

$$\text{weight of siloxane} = 74 * \text{Si}$$

In a similar fashion:

$$\text{weight of sulfone} = 442 * \text{S}$$

Therefore:

$$\text{weight percent siloxane} = 74 * \text{Si} / (74 * \text{Si} + 442 * \text{S})$$

Rearranging yields:

$$\text{weight percent siloxane} = 1 / (1 + 5.97 * (\text{S}/\text{Si}))$$

The above equation converts the S/Si atom ratio to weight percent siloxane. An addition factor is needed to convert the S/Si area ratio into the S/Si atom ratio. Using the XPS quantification factors discussed in Chapter 3 the conversion factors are:

$$(\text{S}/\text{Si})_{\text{atom}} = (\text{S}2\text{p}/\text{Si}2\text{p}) * (348/835)$$

$$(\text{S}/\text{Si})_{\text{atom}} = (\text{S}2\text{p}/\text{Si}2\text{s}) * (418/835)$$

Substituting these factors into the weight percent siloxane equation yields:

$$\text{weight percent siloxane} = 1/(1 + 2.99*(S2p/Si2p))$$

$$\text{weight percent siloxane} = 1/(1 + 3.55*(S2p/Si2s))$$

VITA

Glenn E. Lawson was born in Brooklyn, New York on December 14, 1961. Upon graduation from Tottenville High School in Staten Island, New York in June 1979 he enrolled in the engineering program at Virginia Tech. In September 1981 he married Robin C. Smith in Blacksburg, Virginia. He graduated Cum Laude in Materials Engineering in June 1983. In September 1983 he began graduate studies at Virginia Tech in Materials Engineering with emphasis on polymer materials. In June 1984 he took a position as materials and process engineer with the Lighting Division of Harvey Hubbell, Inc. while continuing to pursue his degree in the evenings and on the weekends. His daughter Monica Carol was born in November 1984. In October 1985 he received his Master of Science degree in Materials Engineering from Virginia Tech.

Glenn E. Lawson